UNIVERSIDADE ESTADUAL PAULISTA "JÚLIO DE MESQUITA FILHO"

FACULDADE DE MEDICINA

Ana Paula Silveira Leite

Comparação entre o uso de sutura e sutura associada ao selante de fibrina (CEVAP) na interação neuromuscular após Lesão Nervosa Periférica

Dissertação apresentada à Faculdade de Medicina de Botucatu, Universidade Estadual Paulista "Júlio de Mesquita Filho", Câmpus de Botucatu, para obtenção do título de Mestre em Bases Gerais da Cirurgia.

Orientadora: Profa. Dra. Selma Maria Michelin Matheus

Botucatu

2018

Ana Paula Silveira Leite

Comparação entre o uso de sutura e sutura associada ao selante de fibrina (CEVAP) na interação neuromuscular após Lesão Nervosa Periférica

Dissertação apresentada à Faculdade de Medicina de Botucatu, Universidade Estadual Paulista "Júlio de Mesquita Filho", Câmpus de Botucatu, para obtenção do título de Mestre em Bases Gerais da Cirurgia.

Orientadora: Profa. Dra. Selma Maria Michelin Matheus

Botucatu

2018

FICHA CATALOGRÁFICA ELABORADA PELA SEÇÃO TÉC. AQUIS. TRATAMENTO DA INFORM.
DIVISÃO TÉCNICA DE BIBLIOTECA E DOCUMENTAÇÃO - CÂMPUS DE BOTUCATU - UNESP
BIBLIOTECÁRIA RESPONSÁVEL: ROSEMEIRE APARECIDA VICENTE-CRB 8/5651

Leite, Ana Paula Silveira.
Comparação entre o uso de sutura e sutura associada ao selante de fibrina (CEVAP) na interação neuromuscular após Lesão Nervosa Periférica / Ana Paula Silveira Leite. - Botucatu, 2018

Dissertação (mestrado) - Universidade Estadual Paulista "Júlio de Mesquita Filho", Faculdade de Medicina de Botucatu
Orientador: Selma Maria Michelin Matheus Capes:
20600003

1. Nervos periféricos - Ferimentos e lesões. 2. Fibrina.
3. Suturas. 4. Adesivo tecidual de fibrina. 5. Nervos - Regeneração.

Palavras-chave: Interação neuromuscular; Lesão nervosa periférica; Selante de fibrina (CEVAP).

Dedicatória

Dedico este trabalho a minha avó Judite,
por estar sempre presente, por me ouvir e apoiar
incondicionalmente e por acreditar em mim quando nem eu
mesma era capaz, te amo infinito vó.

Agradecimentos

Agradeço primeiramente a Deus, pelo dom da vida e por me guiar nesta jornada.

Aos meus pais, Carlos e Rose, pelo apoio e amor incondicional.

À minha irmã, Juliana, minha ouvinte fiel e melhor amiga, obrigada por ser tão presente independente da distância.

Aos meus avós, João e Antonia, Edison e Judite por serem meu porto seguro de carinho e cuidado.

A minha família Cafofo, pelo apoio e companheirismo diário.

A minha orientadora, Professora Drª Selma M. M. Matheus, por toda a experiência e conhecimento compartilhado, e por ser um exemplo de profissional na qual eu me espelho para o futuro.

Ao professor Dr André Luis Filadelpho, pelo auxílio com o protocolo cirúrgico deste estudo e pela extrema atenção de sempre, obrigada.

Ao CEVAP (UNESP/Botucatu) por gentilmente ceder o selante de fibrina para a realização deste trabalho.

Ao programa de Pós-graduação em Bases Gerais da Cirurgia, ao Instituto de Biociências, da UNESP de Botucatu e a UNIPEX, Unidade de pesquisa experimental da Faculdade de Medicina de Botucatu (FMB), pela estrutura e apoio para a realização deste trabalho, e a CAPES pela concessão da bolsa de estudos.

Á todos os professores e funcionários do departamento de Anatomia pelo auxílio e companheirismo de sempre.

Agradeço também aos funcionários da Unipex, cujo conhecimento e auxílio foram indispensáveis para realização deste estudo, em especial ao Bardella, Zé, Robson, Sílvio e Diego por todo o cuidado com os animais utilizados neste estudo.

Aos colegas do laboratório de Anatomia, pela amizade, apoio e companheirismo diários.

Em especial a Carina, por ser a melhor parceira de laboratório que alguém poderia desejar e por ser também amiga para todos os momentos.

Agradeço ao Professor Carlos Roberto Padovani pelo auxílio com as análises estatísticas deste trabalho.

Aos membros das bancas de qualificação e defesa pela disposição e colaborações fundamentais para este trabalho.

Aos animais desse experimento pelas vidas doadas, as quais espero ter feito valia no desenvolvimento deste trabalho.

Muito obrigada!

Epígrafe

"Mire a lua. Mesmo se você errar,
você ficará entre as estrelas."
(Les Brown)

RESUMO

Os nervos periféricos são comumente acometidos por lesões que acarretam interrupção do impulso nervoso. Dentre as causas mais comuns, estão: traumas, estiramento, pinçamento, compressão e esmagamento, resultando em comprometimento do sistema neuromuscular. A recuperação tanto morfológica quanto funcional após este tipo de lesão raramente é completa, sendo um desafio para clínica médica. A maior parte da literatura tem como foco o estudo da recuperação nervosa e muscular, havendo poucas referências em relação às junções neuromusculares (JNM). Além disso, outros procedimentos vêm sendo testados como uma forma de minimizar os danos causados pelo uso da sutura. Dentro desta proposta este estudo teve como objetivo avaliar o uso do selante de fibrina (CEVAP) associado ao número reduzido de pontos (1 ponto), quando comparado a sutura convencional (3 pontos), após lesão do nervo isquiático. Foram utilizados 36 ratos Wistar machos adultos, divididos em 4 grupos experimentais: Controle (C), Desnervado (D); Sutura (S) e Sutura + Selante de Fibrina (SFS). No grupo C, foi realizada apenas incisão superficial no antímero direito, afastamento da musculatura e localização do nervo isquiático. No grupo D foi realizada neurotmese do nervo isquiático (gap de 6 mm). No grupo S foi realizada transecção completa do nervo isquiático direito e após 7 dias foi efetuada anastomose epineural do mesmo. No grupo SFS, a reconstrução nervosa foi realizada com um ponto de sutura, seguida da aplicação do selante de fibrina CEVAP (Centro de Estudos de Venenos e Animais Peçonhentos) - UNESP – Botucatu. Antes da realização dos procedimentos cirúrgicos e nos 15°, 30°e 60° dia após a secção e sepultamento nervoso foi realizada análise no Catwalk de todos os animais de acordo com os grupos experimentais. Decorrido o período experimental (60° dia) os animais foram anestesiados para análise eletroneuromiografica e a seguir eutanasiados. Os nervos isquiáticos, ramos musculares do nervo tibial para o músculo sóleo e os músculos sóleos dos antímeros direitos, foram coletados e submetidos a: a) análise morfológica (esterase inespecífica) e morfométrica das JNMs através de microscopia de luz e de transmissão; b) análise morfológica e morfométrica das fibras musculares (HE); c) frequência dos tipos de fibra muscular (Fast e Slow); c) quantificação da porcentagem de colágeno no tecido muscular; d) expressão proteica: PaX7 e PCNA (Western Blotting); e) análise morfológica e morfométrica dos nervos(tetróxido de ósmio). As análises eletroneuromiográficas revelaram que os valores de amplitude e latência dos grupos S e SFS foram semelhantes entre si, sendo indicativos de regeneração. As análises do Catwalk indicaram que houve déficit funcional em todos os grupos lesão (D, S e SFS), ao final do período experimental. A análise morfológica do ramo muscular do nervo tibial mostrou que os grupos S e SFS se aproximaram do C, e os valores da razão G se mantiveram dentro do padrão de normalidade. A mesma análise no nervo isquiático mostrou valores superiores referentes á área e diâmetro dos axônios e fibras nervosas no grupo SFS em relação ao grupo S, com todos os grupos apresentando também a razão G dentro da faixa de normalidade. Nos grupos S e SFS houve aumento do peso muscular, da área das fibras musculares e diminuição da porcentagem de colágeno em relação ao grupo D. Nas JNMs houve restabelecimento dos botões sinápticos e indicativo de aumento da área das mesmas. Houve aumento da frequência de fibras Fast nos grupos lesão, havendo também presença de “type grouping” nos mesmos. A quantificação das proteínas PaX7 e PCNA não mostrou diferença entre os grupos. Os resultados do nosso estudo permitiram concluir que houve um restabelecimento do impulso nervoso, além da regeneração axonal, que foi tão eficiente no grupo SFS quando comparado ao grupo S, com valores superiores no grupo SFS na área da lesão (nervo isquiático). Sendo indicativo de um efeito protetor no local da lesão devido ao uso de selante de fibrina heterólogo. Pode-se considerar que o uso deste selante permite a diminuição do número de pontos reduzindo o trauma causado pela agulha, e acelerar a prática cirúrgica. Portanto, o selante de fibrina heterólogo deve ser considerado na reconstrução nervosa após a lesão do nervo periférico.

Abstract

Peripheral nerves are commonly affected by injuries that lead to interruption of the nerve impulse. Among the most common causes are: trauma, stretching, pinching, compression and crushing, resulting in impairment of the neuromuscular system. Both morphological and functional recovery after this type of injury is rarely complete and a challenge for medical practice. Most of the literature focuses on the study of nerve and muscle recovery, with few references to neuromuscular junctions (NMJs). In addition, other procedures have been tested as a way to minimize the damages caused by the use of suture. The aim of this study was to evaluate the use of fibrin selant (CEVAP) associated to reduced number of stitches (1 point) when compared to conventional suture (3 stitches) after ischiatic nerve injury. Thirty-six male adult Wistar rats were divided into four experimental groups: Control (C), Desnervate (D), Suture (S) and Suture + Fibrin Sealant (SFS). In group C, an only superficial incision was made in the right antimer, followed by distance from the musculature and location of the ischiatic nerve. In group D, ischiatic nerve neurotmesis (6 mm gap) was performed. In group S, a complete transection of the right ischiatic nerve was carried out and after 7 days an epineural anastomosis of the ischiatic nerve was performed. In the SSF group, the nerve reconstruction was performed with one suture point, followed by the application of CEVAP fibrin sealant (Unesp- Botucatu Center for the Study of Venoms and Venomous Animals). Before the surgical procedures and at the 15th, 30th and 60th day after sectioning and nervous burial, Catwalk analysis of all animals was made according to the experimental groups. After the experimental period (60th day) the animals were anesthetized for electromyography and then euthanized. The ischiatic nerves and the tibial nerve-muscle branch to the soleus muscle and the right antimer of soleus muscle were collected and submitted to a) morphological (non-specific esterase) and morphometric analysis of NMJs by light and transmission microscopy; b) morphological and morphometric analysis of muscle fibers (HE); c) quantification of the percentage of collagen in muscle tissue (Picrossirius Red); d) protein expression: PaX7 and PCNA (Western Blotting); e) morphological and morphometric analysis of the nerves (osmium tetroxide). Electromyography analyzes revealed that the amplitude and latency values of the S and SFS groups were similar to each other and were indicative of regeneration. Catwalk analysis indicated that there was a functional déficit in all groups presenting injury (D, S and SFS) at the end of the experimental period. The morphological analysis of the tibial nerve-muscle branch showed that the S and SFS showed to be similar to C group, and the G ratio remained within the normal range. The same analysis in the sciatic nerve showed higher values referring to the area and diameter of the axons and nerve fibers in the SFS group in relation to the S group, with all groups also presenting the G ratio within the normal range. In the S and SFS groups there was an increase in muscle weight, in the area of muscle fibers and a decrease in the percentage of collagen in relation to group D. In the NMJs there was a reestablishment of the terminal boutons and an indication of an increase in its area. There was an increase in the frequency of Fast fibers in the lesion groups, and there was a type grouping pattern of distribution in them as well. Quantification of the PaX7 and PCNA proteins showed no difference between the groups. Our study results allowed us to conclude that there was a reestablishment of the nerve impulse, in addition to axonal regeneration, which was as efficient in the SFS group when compared with the S group, with superior values in the SFS in the lesion area (ischiatic nerve). It is an indicative of a protective effect at the lesion site due to the heterologous fibrin sealant use. It can be considered that the decrease in the number of stitches is able to reduce the trauma caused by the needle, as well as accelerating the surgical practice. So the heterologous fibrin sealant used in nerve reconstruction should be considered after peripheral nerve injury.

Lista de Abreviaturas

ACh- Acetilcolina

C- Controle

CEVAP- Centro de Estudos de Venenos e Animais Peçonhentos

CEUA- Comissão de Ética no Uso de Animais

D-Desnervado

DAB- Diaminobenzidina 3,3

EPL- print lengh lado lesionado

ETS- toe spread lado lesionado

FMB- Faculdade de Medicina de Botucatu

g- Gramas

GAPDH- Gliceraldeído-3-fosfato desidrogenase

HE- Hematoxilina & Eosina

H_2O_2- Peróxido de Hidrogênio

IB- Instituto de Biociências

IFF- Índice Funcional do Fibular

JNM- Junção Neuromuscular

Kg- Kilogramas

LNPs- Lesões Nervosas Periféricas

mg- miligramas

µL- microlitros

µm- micrómetros

NPL- print lengh lado normal

NTS- toe spread lado normal

PaX7- Paired Box Protein

PCNA- Proliferating Cell Nuclear Antigen

S- Sutura

SFS- Sutura + Selante de Fibrina

TBSt- Tris-buffered saline with Tween

UNESP- Universidade Estadual Paulista “Júlio de Mesquita Filho”

UNIPEX- Unidade de Pesquisa Experimental- Faculdade de Medicina de Botucatu

Sumário

Sumário

1.0 INTRODUÇÃO

Os músculos estriados esqueléticos são inervados por axônios cujos corpos celulares estão localizados na coluna anterior da medula espinal; estes axônios percorrem longas distâncias até atingirem as fibras musculares. A sinapse química de contato entre o axônio motor e a fibra muscular esquelética, é a estrutura funcionalmente especializada denominada de Junção Neuromuscular (JNM) a qual é morfologicamente distinta, sendo responsável pela transmissão de um sinal elétrico do neurônio motor para a fibra muscular promovendo a contração muscular (Malomouzh, 2012; Tintignac *et al.*, 2015).

Morfologicamente, as JNMs são formadas por três compartimentos: o compartimento pré-sináptico, onde estão presentes a terminação nervosa com as vesículas contendo o neurotransmissor responsável, a acetilcolina (ACh) e as células de Schwann, específicas desta região, denominadas células de Schwann terminais; o compartimento extracelular (fenda sináptica), preenchido pela lâmina basal, estando também ali a enzima acetilcolinesterase, responsável pela quebra da acetilcolina após a contração muscular; e o compartimento pós-sináptico, que compreende o sarcolema da fibra muscular com as dobras juncionais, onde se encontram os receptores de acetilcolina e o sarcoplasma que proporciona suporte estrutural e metabólico para a região pós-sináptica (Engel, 2008; Malomouzh, 2012).

Para que ocorra a contração muscular a interação nervo músculo deve estar íntegra. Vários fatores podem provocar alterações nas JNMs, dentre eles as lesões nervosas periféricas (LNP), as quais resultam em uma perda da conexão entre o axônio e o músculo, levando a uma degeneração dessas estruturas (Ruven *et al.*, 2017).

As LNPs são comumente resultantes de traumas após acidentes automobilísticos, lacerações com materiais cortantes e até mesmo em decorrência de quedas (Robinson, 2000). Considerado um quadro clínico comum, incide em aproximadamente 13,9 pessoas a cada 100 mil anualmente (Asplund *et al.*, 2009), e pode causar perdas sensoriais e ou motoras, além de dor crônica (Sullivan *et al.*, 2016; Uyanikgil *et al.*, 2017).

Seddon (1942), introduziu uma classificação para as lesões nervosas, onde a neuropraxia é caracterizada pela interrupção da condução nervosa por uma lesão na bainha de mielina, sem descontinuidade axonal, apresentando recuperação rápida e

completa. Na axonotmese ocorre um bloqueio da condução nervosa decorrente de uma perda parcial na continuidade do axônio, sendo seguida do processo de degeneração Walleriana distal à lesão, a recuperação funcional nestes casos depende do crescimento axonal, e ocorre mais comumente associada a lesões por esmagamento e fraturas ósseas, sendo que a recuperação total é menos provável do que na neuropraxia. Já a neurotmese ocorre quando há transecção completa do nervo, havendo bloqueio da condução elétrica sendo então, considerada a forma mais grave de lesão nervosa. Este tipo de lesão não apresenta recuperação funcional espontânea, tornando-se necessária intervenção cirúrgica.

Quando os neurônios motores são desligados de suas fibras musculares por lesão de um nervo periférico, eles frequentemente se regeneram e se reconectam com as fibras musculares. Os axônios em regeneração, normalmente, seguem os tubos endoneurais ("tubos das células de Schwann") que anteriormente ocupavam (Nguyen *et al.*, 2002). Quando os axônios se aproximam dos locais das sinapses, há frequentemente uma remodelação desses contatos. O grau dessa remodelação depende de quão rapidamente os sítios são reinervados; reinervação rápida leva a uma melhor remodelação, enquando a reinervação tardia, provoca mudanças mais profundas no sítio sináptico, dificultando assim a regeneração (Rich e Lichtman, 1989).

Essa remodelação envolve uma reação inflamatória, onde, as células satélites são ativadas para reconstrução muscular, atuando na proliferação, diferenciação e fusão de novas miofibrilas (Charge e Rudnicki, 2004). Sendo ainda necessária, a presença de uma reinervação com JNMs maduras para as recém-formadas miofibrilas completarem seu processo de diferenciação e recuperação da força muscular (Lin *et al.*, 2008).

Embora haja um potencial de regeneração espontânea, a recuperação funcional após lesão nervosa é limitada em adultos (Ray e Mackinnon, 2010). Vários são os fatores limitantes desta recuperação: conexões inadequadas entre os axônios e o órgão-alvo; aderências teciduais e contraturas musculares decorrentes de longos períodos de imobilização e atrofia (Alluin *et al.*, 2009).

Dentre as alterações morfológicas, decorrentes deste tipo de lesão; nas fibras musculares, são observados decréscimo da secção transversal das mesmas, redução do número de mionúcleos e de células satélites, bem como redução do próprio peso do músculo desnervado (Gutmann e Zelena, 1962; Anzil e Wernig,

1989; Borisov e Carlson, 2000; Schmalbruch e Lewis, 2000; Ma *et al.*, 2007); além de progressiva atrofia e fibrose (Gutmann, 1948; Fu e Gordon, 1995; Burnett e Zager, 2004); ultraestruturalmente estão presentes desorganização de sarcômeros, dano mitocondrial e vacuolização (Moimas *et al.*, 2013); Os tipos de fibras musculares também se alteram na desnervação, onde músculos de padrão predominantemente oxidativo, passam a apresentar um padrão mais equivalente de fibras oxidativas e glicolíticas. Já nos músculos de padrão predominantemente glicolítico, o número de fibras oxidativas tendem a aumentar (Pette e Vrbova, 1985; Windisch *et al.*, 1998; Loughna e Morgan, 1999).

Na fibra nervosa, logo após a secção do nervo se inicia a degeneração da bainha de mielina pelos macrófagos (Siemionow e Sonmez, 2007). No coto distal do axônio ocorre um processo autolítico, que leva a fragmentação do axônio; a área de contato sináptica é invadida por células de Schwann, que irão influenciar o crescimento axonal, através da ação de fatores neurotróficos a partir do coto proximal (Lundborg, 1987; Lundborg, 2000). Os axônios, a partir do nodo de Ranvier, começam a emitir ramificações em direção ao coto distal, continuando seu crescimento ao longo das bandas de Büngner, as quais são formadas pelas células de Schwann que se dividem e se organizam no interior de tubos de membrana basal, de forma linear (Lundborg, 1987; Ferreira, 2001; Rodrigues e Silva, 2001). Assim nos nervos pós-lesão poucas fibras nervosas estão presentes, normalmente em degeneração, de formato irregular, com diâmetro variado e associadas a grande quantidade de tecido conjuntivo (Maciel *et al.*, 2013; Buchaim *et al.*, 2015).

Já em relação às JNMs foi demonstrado que a desnervação em longo prazo, leva a uma desorganização das mesmas, havendo redistribuição dos receptores de acetilcolina através da fibra muscular (Hartzell e Fambrough, 1972; Frank *et al.*, 1975; Steinbach, 1981; Kurimoto *et al.*, 2015). Tem sido descrito ainda aumento da área e fragmentação da JNM, além de um aumento na profundidade da goteira sináptica (Ma *et al.*, 2007).

Com a finalidade de busca da reinervação e restituição da função nervosa e muscular, nos últimos dez anos, várias estratégias vêm sendo utilizadas (Ray e Mackinnon, 2010); Que em sua maioria fazem referência a tratamentos cirúrgicos baseados na reconstrução anatômica, auto-enxerto e guia de nervos, e nem sempre são capazes de restabelecer a força muscular e a capacidade de contração anterior à lesão (Bentolila *et al.*, 1999; Kim *et al.*, 2003; Kang *et al.*, 2011; Griffin *et al.*, 2013).

Quando a lesão é do tipo neurotmese, com preservação dos cotos nervosos, o padrão ouro de reconstrução utilizado é a neurorrafia término-terminal com uso de sutura (Rafijah *et al.*, 2013; Wu *et al.*, 2014). Este tipo de neurorrafia só é possível de ser realizada em situações onde, não há tensão para aproximação dos cotos (Biscola *et al.*, 2017), quando a tensão está presente, outras técnicas são utilizadas; entre elas: neurorrafia término-lateral (Viterbo *et al.*, 1992), uso de enxertos e conduites (Grinsell e Keating, 2014).

Embora seja considerada a técnica ideal para este tipo de lesão, o uso de sutura para reconstrução nervosa pode causar reações inflamatórias, incluindo a formação de granulomas e neuromas, levando nesse caso a um quadro de dor crônica (Nakamura *et al.*, 2004; Chimutengwende-Gordon e Khan, 2012); Uma forma de minimizar os danos causados pelo uso da sutura seria a redução dos pontos utilizados para reconstrução (Biscola *et al.*, 2017). Neste sentido a cola de fibrina surge como uma metodologia adjuvante, apresentando boa capacidade na adesão de tecidos e vem sendo amplamente utilizada na medicina desde a década de 70 (Isaacs *et al.*, 2008). Porém apresenta a desvantagem de apresentar em sua composição, o fibrinogênio derivado de sangue humano, o qual pode causar reações adversas (Nakamura *et al.*, 2004; Chimutengwende-Gordon e Khan, 2012). Seu uso junto à sutura possibilita a redução do número de pontos, podendo até a substituir, mas ainda há aspectos controversos na literatura.

Há relatos de que a associação entre a cola de fibrina (comercial) e a sutura é igualmente benéfica quando comparada ao uso apenas da cola, sugerindo ainda que o uso da cola promova maior regeneração axonal, sendo vantajoso quando comparado com a sutura (Martins *et al.*, 2005), além de promover aumento na área das fibras nervosas lesionadas (Felix *et al.*, 2013). Outros trabalhos relatam, porém que a regeneração nervosa é superior após o uso de sutura quando comparado à cola (Temple *et al.*, 2004; Farrag *et al.*, 2007; Nishimura *et al.*, 2008). Estes estudos destacam principalmente uma menor resistência da cola à ruptura durante as primeiras semanas pós-operatórias (Nishimura *et al.*, 2008).

O Centro de Estudos de Animais Peçonhentos (CEVAP- UNESP- Botucatu-SP) desenvolveu um novo adesivo de fibrina derivada do veneno da serpente *Crotalus durissus terrificus*, sendo considerado um selante biológico e biodegradável, que não produz reações adversas. Por ser livre de sangue humano, não é transmissor de doenças infecciosas, além de ter uma boa capacidade adesiva,

podendo ser utilizado junto a procedimentos de sutura tradicional (Barros *et al.*, 2009). Em sua composição o crioprecipitado contendo fibrinogênio e fatores de coagulação são derivados do sangue de búfalo, e a trombina responsável é substituída pela giroxina, uma proteína trombina-like capaz de clivar fibrinogênio em monômeros de fibrina (Ferreira, 2014). A utilização deste selante no reparo de LNP vem apresentando resultados bastante promissores (Vicente *et al.*, 2008; Buchaim *et al.*, 2015).

Mesmo com os avanços nos procedimentos cirúrgicos, as reconstruções nervosas resultam apenas em torno de 51% de recuperação motora (Sakuma *et al.*, 2016). Enquanto muitos trabalhos mostram que há regeneração morfológica do nervo e do músculo isso não está associado a uma recuperação funcional, ainda que haja regeneração axonal, com as JNMs em aparência morfológica normal, a falha na ativação elétrica muscular persiste (Sakuma *et al.*, 2016). Assim além do nervo e das fibras musculares, a JNM também deve ser considerada nestes tipos de análises, bem como a resposta funcional resultante dessas interações. O selante de fibrina surge como um potencial adjuvante ao processo de regeneração, quando associado à sutura, permitindo redução do número de pontos e atuando como um suporte, contribuindo para o microambiente de crescimento axonal (Biscola *et al.*, 2017).

Diante do exposto o objetivo deste trabalho foi avaliar a associação do selante de fibrina (CEVAP) com a sutura, quando comparado ao uso exclusivo da sutura, após lesão do nervo isquiático. Onde foram avaliados aspectos morfológicos e funcionais da interação neuromuscular.

Objetivos específicos:

- Análise funcional (Catwalk e Eletroneuromiografia).
- Análise morfológica e morfométrica do nervo isquiático e do ramo muscular do nervo tibial para o músculo sóleo
- Análise morfológica e morfométrica das fibras musculares (HE) do músculo sóleo
- Quantificação da porcentagem de colágeno junto ao músculo sóleo (Picrossirius Red)
- Frequência das fibras musculares Fast e Slow (Imunohistoquímica)

- Análise morfológica e morfométrica das JNMs através de microscopia de luz (esterase inespecífica)
- Análise ultraestrutural das fibras musculares do músculo sóleo e das JNMs associadas
- Expressão proteica (Western Blotting) do PCNA (proliferação celular) e PAX7 (células satélites).

2.0 Material e Métodos

Foram utilizados 36 ratos Wistar adultos machos (CEUA FMB 1172/2016), provenientes do Biotério Central da UNESP, com peso médio entre 300 – 400g. Durante todo o experimento, os animais foram mantidos em ambiente com controle de temperatura (24±2ºC) e de fotoperíodo (12h:12h). Os animais foram aleatoriamente divididos em 4 grupos experimentais:

1-Controle (C); 2- Desnervado (D); 3- Sutura (S); 4- Sutura + Selante de Fibrina (SFS).

Os ratos foram então anestesiados através de injeção intraperitoneal de Ketamina (Dopalen – 90mg/kg) e Xilazina (Rompun – 10mg/kg). Após tricotomia do membro inferior direito, os animais foram posicionados em decúbito ventral, mantendo-se as patas dianteiras e traseiras em abdução. Foi realizada a antissepsia com álcool-iodado, seguida de incisão sobre a face lateral da coxa, desde a altura do trocânter maior até o joelho e os nervos isquiáticos direitos foram expostos (Figura 1 A e B). Nos animais do grupo Desnervado (D), Sutura (S) e Sutura + Selante de Fibrina (SFS), de forma padronizada, a cerca de 3 mm distal a sua emergência, foi realizada uma lesão nervosa por transecção completa do nervo (Figura 1 C). Nos animais do grupo D a fim de evitar regeneração espontânea, foi removido um fragmento de 6 mm do nervo isquiático. Após neurotmese os cotos proximais e distais foram invertidos em 180 graus e fixados a musculatura adjacente, com pontos simples com fio de nylon Mononylon 5-0, Polysuture. Após este procedimento os tecidos moles foram suturados com pontos simples com fio de nylon Mononylon 3-0, Polysuture. Nos animais do grupo C (controle) após localização do nervo isquiático a pele foi suturada. Terminado o procedimento os animais de todos os grupos foram mantidos sob aquecimento até a recuperação e, ao acordarem receberam solução contendo dipirona sódica via gavagem.

Decorridos 7 dias da neurotmese, com um quadro de degeneração já estabelecido, os animais dos grupos S e SFS passaram por microcirurgia reconstrutiva para reparo do nervo isquiático. Após a anestesia e tricotomia, os animais foram posicionados em decúbito ventral, foi efetuada nova incisão, e os cotos antes fixados a musculatura adjacente foram submetidos à neurorrafia término-terminal (Figura 1 D). A opção por esse período de espera até a reconstrução nervosa-7 dias, foi escolhida visando observar a ação do selante após o início do processo de degeneração Walleriana, podendo ainda ser considerado como um modelo de comparação para a prática clínica, onde a reconstrução nervosa (conexão dos cotos) por vezes é adiada em detrimento a traumas de maior urgência.

No grupo Sutura, os cotos foram ligados por anastomose epineural com três pontos simples de monofilamento nylon (Mononylon 7-0, Polysuture). Já no grupo Sutura + Selante de Fibrina (SFS), a conexão entre os cotos proximais e distais se deu através de 1 ponto de sutura, associado a 100 µL de selante de fibrina, gentilmente cedido pelo CEVAP, Brasil, cujos componentes e fórmula de aplicação constam das suas patentes (Números do registro: BR1020140114327 e BR1020140114360) (Figura 1E). No momento do uso os componentes foram previamente descongelados, reconstituídos, misturados e aplicados sobre o local da lesão (Gasparotto, V. P. *et al.*, 2014).

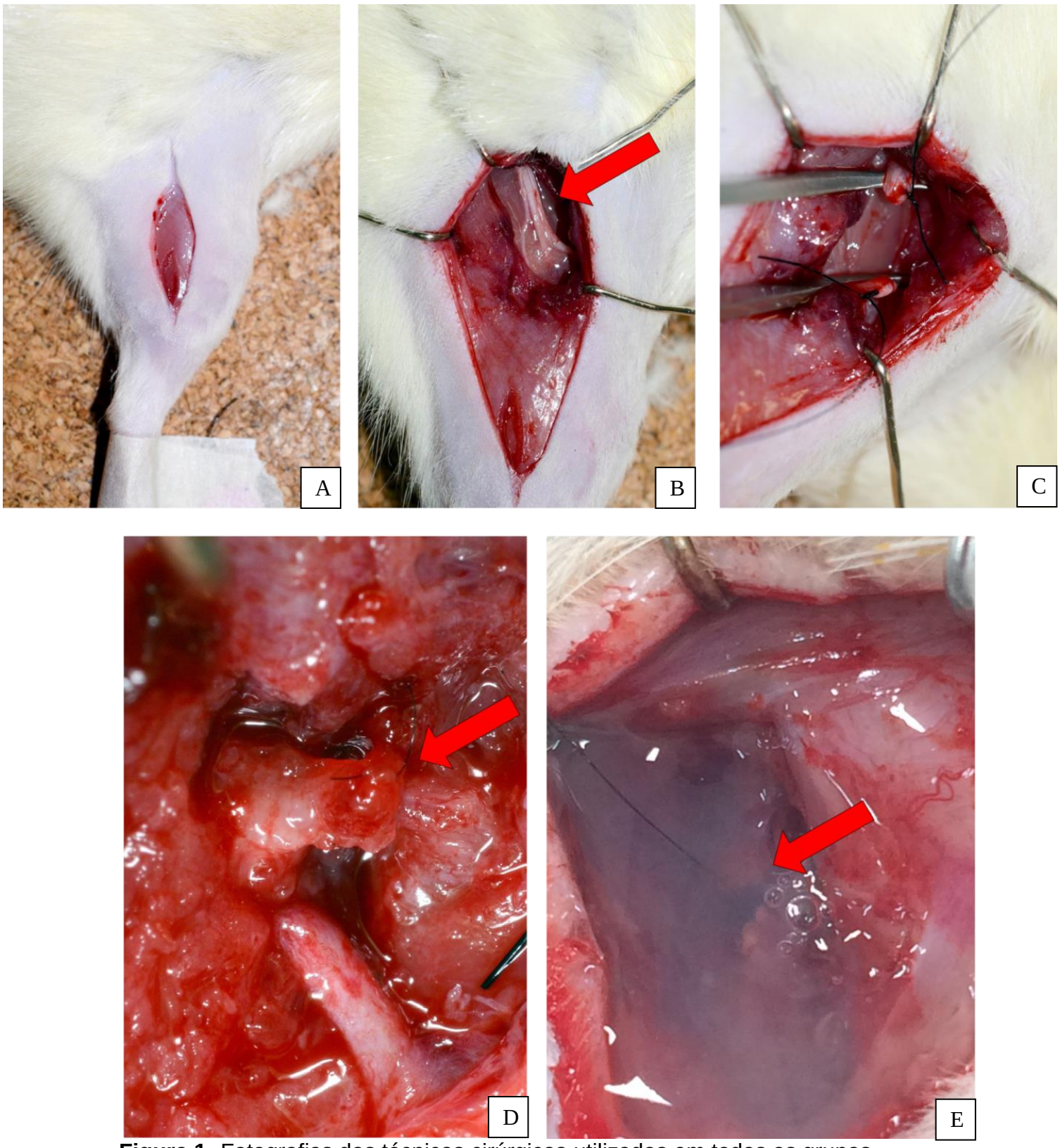

Figura 1: Fotografias das técnicas cirúrgicas utilizadas em todos os grupos experimentais. A- Incisão. B- localização do Nervo Isquiático (seta). C-Neurotmese. D- Detalhe da Neurorrafia após 7 dias de lesão(seta-sutura). E- Detalhe da neurorrafia associada ao selante de fibrina (seta- coágulo formado pelo selante).

Após a realização do reparo cirúrgico, os tecidos moles foram suturados com pontos simples com poliester siliconado nº 5, os animais ficaram sob aquecimento até a recuperação e ao acordarem foi oferecida a eles solução contendo dipirona sódica via gavagem. Nos dois dias consecutivos, a cada 12 horas, foi mantida a administração do analgésico. A lesão por transecção completa foi preferida neste estudo a uma lesão por esmagamento, pois esta preserva a estrutura de sustentação do nervo, aumentando o prolongamento axonal, visto que os tubos neurais estão em continuidade, facilitando, assim, a regeneração. Decorrido o período experimental (60 dias- última cirurgia), todos os animais foram pesados e anestesiados através de injeção intraperitoneal de Ketamina (Dopalen – 90mg/kg) e Xilazina (Rompun – 10mg/kg), para realização da eletroneuromiografia e em seguida eutanasiados com tiopental sódico. Os ramos musculares do nervo tibial para o músculo sóleo e os músculos sóleos direitos (Figura 2) foram dissecados e devidamente preservados para o procedimento das diferentes análises. Os nervos isquiáticos também foram coletados (distalmente a lesão).

Figura 2: Fotografia da pata direita no momento da coleta. Seta- ramo muscular do nervo tibial para o músculo sóleo. Asterisco- músculo sóleo.

2.1 Avaliação da Marcha através do aparelho "Catwalk" (n=9)

Antes da realização dos procedimentos cirúrgicos, e nos 15º, 30º e 60º dias após a secção e reconstrução nervosa foi realizada análise no Catwalk XT 9.1-Noldus (Unipex/FMB-Botucatu) de todos os animais de acordo com os grupos experimentais. Inicialmente os animais foram treinados (uma ou duas vezes) a caminhar no dispositivo utilizado para avaliação da marcha. O estudo se baseou nas pegadas e marcha do animal, de forma estática e dinâmica, baseadas em duração, orientação e coordenação dos movimentos entre as patas. Trata-se de um sistema de análise automatizado da marcha, no qual os animais foram colocados para andar em uma plataforma de vidro iluminada, o contato da pata com a superfície do vidro resulta em uma imagem nítida e brilhante da pegada. A plataforma de vidro é motorizada por uma câmara de vídeo colocada sob a plataforma e ligada a um computador equipada com um software de aquisição de vídeo e análise das pegadas.

Os critérios adotados para que uma caminhada fosse considerada adequada para o experimento foram:

1- Que a caminhada dure ao menos 0,50 segundos.

2-Que a caminhada não exceda 30 segundos em tempo.

3- Que o número mínimo de pegadas seja de quatro, completas.

4- A variação na velocidade permitida será de 60%.

A intensidade do sinal depende da área da pata em contato com a plataforma e aumenta com a pressão aplicada pela pata.

Os parâmetros avaliados foram:

1- Índice funcional do fibular.

2-"Stand"- tempo de contato da pata com o vidro.

3- Contato ou medida da área de contato máximo.

4- Área da pegada.

Os valores do Índice funcional do fibular foram obtidos através da seguinte fórmula: IFF=174.9 ((EPL-NPL)/NPL) + 80.3 x (ETS-NTS)/NTS) - 13.4, onde E se refere ao lado lesionado e N ao lado não lesionado, a sigla TS se refere a distância entre o primeiro e o quinto dedos (toe spread) e a sigla PL a distância entre o terceiro dedo e o calcanhar (print lenght) (Bain *et al.*, 1989).

Para os demais parâmetros: os resultados foram expressos em forma de média da razão dos lados lesionado/não lesionado das impressões plantares, visando analisar de forma mais completa a marcha do animal.

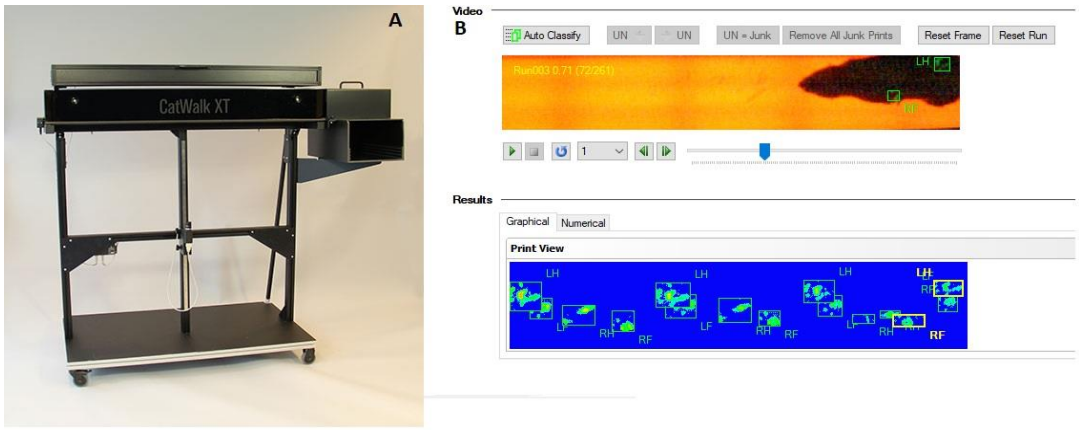

Figura 3: A- Plataforma Catwalk com câmera acoplada (www.noldus.com/Catwalk-XT/specifications). B- Print Screen das análises realizadas junto ao software.

2.2 Eletroneuromiografia (n=9)

Para esse estudo foi utilizado eletromiógrafo da marca Sapphire II 4ME. Após a anestesia, conforme descrito anteriormente, os animais foram imobilizados em decúbito ventral e foram realizadas tricotomia e antissepsia do membro posterior direito. A incisão no membro posterior direito foi realizada para expor o nervo isquiático, além do músculo tibial cranial. No centro do músculo tibial cranial foi implantado o eletrodo ativo (preto), o eletrodo de referência (vermelho) foi implantado próximo ao tendão de inserção do músculo e o eletrodo cinza (dispersivo) introduzido em um local distante da região do teste, no tronco. O eletrodo de estimulação bipolar que deflagrou o impulso elétrico foi posicionado diretamente sobre o nervo isquiático, de modo que a estimulação foi realizada proximal à neurorrafia, possibilitando a propagação dos impulsos elétricos através da mesma. Os eletrodos registraram em conjunto amplitude e latência do potencial de ação muscular em cada estímulo dado.

2.3 Análise morfológica e morfométrica do nervo isquiático e do ramo muscular do nervo tibial para o músculo sóleo (n=5)

Os nervos isquiáticos (distal a lesão) e os ramos musculares do nervo tibial para os músculos sóleos direitos foram expostos, coletados e em seguida foram submetidos à fixação e coloração com tetróxido de ósmio a 1%. Após 24 horas, os exemplares seguiram a rotina do laboratório de histologia do Departamento de Anatomia/IB/UNESP/Botucatu. Foram obtidas secções transversais dos nervos de cerca de 2um de espessura e confeccionadas lâminas histológicas, com as quais foi realizada análise morfométrica dos nervos. Para isso, foram obtidas imagens através do analisador de imagens Olympus Bx41(câmera SC30), do Departamento de Anatomia, Instituto de Biociências – UNESP - Campus de Botucatu. Para o nervo isquiático foram utilizadas imagens de 5 campos aleatórios,e para o ramo muscular do nervo tibial para o músculo sóleo a totalidade do mesmo foi utilizada.Para cada grupo foram obtidas imagens 1000 x com óleo de imersão as quais foram submetidas à análise através do software “Sigma Scan Pro 5”(Figura 4). Através desta análise foi obtido: o número, diâmetro e área dos axônios e fibras nervosas, os diâmetros do axônio e da fibra nervosa, e a partir destes foram calculados a espessura da bainha de mielina e Razão G, utilizando as seguintes fórmulas:

$$\text{Diâmetro médio axônios} = \frac{\sum \text{diâmetro axônios}}{n^{o}\ \text{axônios}}$$

$$\text{Diâmetro médio fibras} = \frac{\sum \text{diâmetro fibras}}{n^{o}\ \text{fibras}}$$

$$\text{Espessura da bainha mielina} = \frac{\text{diâmetro da fibra - diâmetro do axônio}}{2}$$

$$\text{Razão G} = \frac{\text{diâmetro do axônio (média)}}{\text{diâmetro da fibra (média)}}$$

A quantificação das fibras nervosas e dos axônios foi calculada a partir da somatória do número dos mesmos obtidos nos 5 campos aleatórios em objetiva de 100x. A fórmula a seguir demonstra como foi feito o cálculo da estimativa do número de fibras nervosas e de axônios em cada nervo .

$$\text{Estimativa Número Total de Axônios} = \frac{\Sigma\ \text{número de axônios X 100}}{5\ \text{(porcentagem da amostra)}}$$

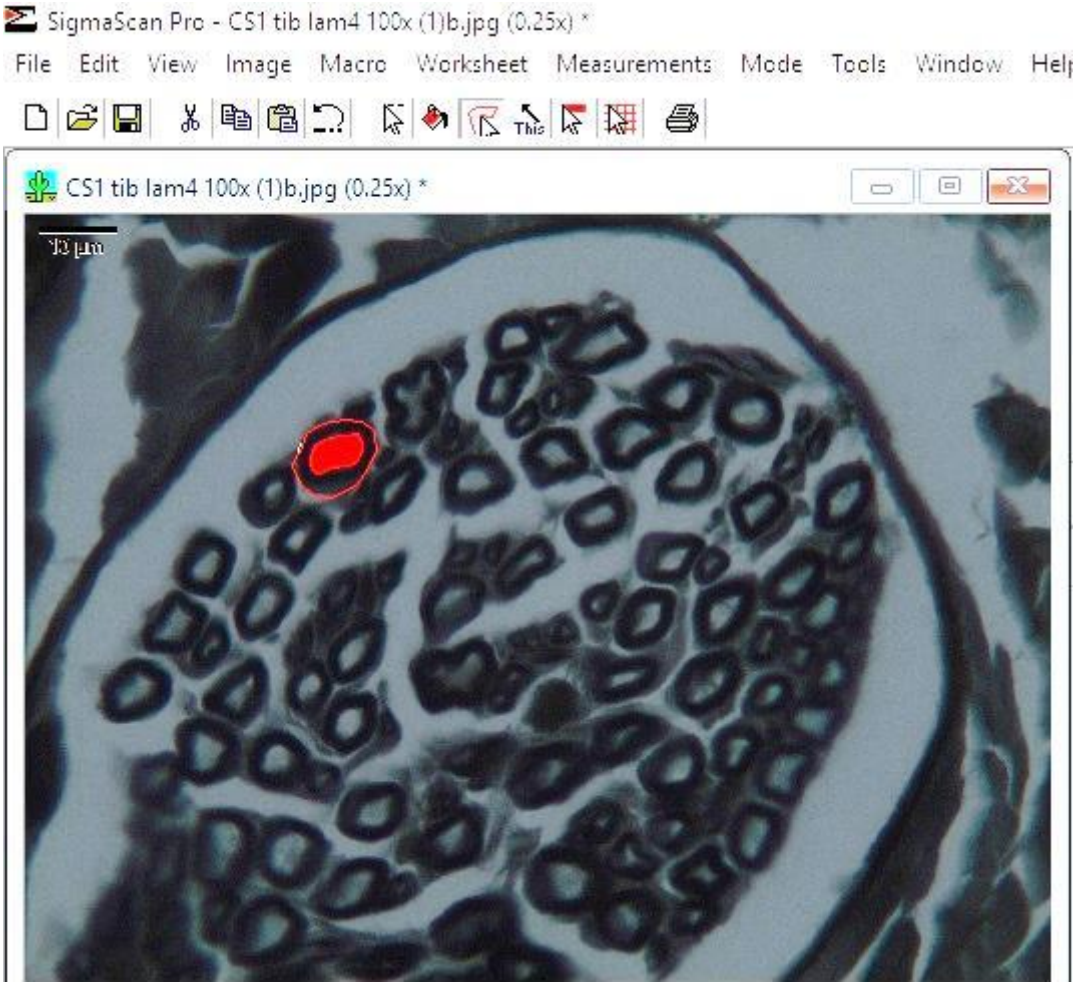

Figura 4: Print Screen da análise morfométrica do ramo muscular do nervo tibial para o músculo sóleo Medidas do axônio (preenchimento vermelho) e da fibra nervosa (contorno vermelho).

2.4 Análise das fibras musculares e porcentagem de colágeno (n=5)

Após congelamento da porção proximal dos músculos sóleos, foi realizada microtomia em criostato (8 µm), e confeccionadas 4 lâminas para cada animal de cada grupo experimental. Cada uma delas foi submetida respectivamente à coloração de Hematoxilina e Eosina (HE), Picrossirus Red e Imunohistoquímica para fibras Fast e Slow. As lâminas confeccionadas foram fotografadas no aumento de 200X através do microscópio Olympus Bx41(câmera SC30).

2.4.1 Análise morfológica e morfométrica das fibras musculares (HE) do músculo sóleo

A primeira lâmina foi submetida à coloração de Hematoxilina e Eosina (HE). Para esta análise foram utilizadas em torno de 200 fibras musculares selecionadas a partir de 3-4 campos aleatórios. Esta quantificação foi realizada através do software livre “Image J" (Schneider *et al.*, 2012).

2.4.2 Quantificação da porcentagem de colágeno presente no músculo sóleo (Picrossirius Red)

A segunda lâmina foi submetida à coloração de Picrossirius Red, onde o colágeno foi marcado em vermelho, e as fibras musculares em amarelo. A porcentagem de colágeno no tecido muscular foi obtida através do software Leica QWin, onde as áreas em vermelho eram detectadas automaticamente pelo software para a obtenção da porcentagem de colágeno.

2.4.3 Frequência das fibras musculares Fast e Slow (Imunohistoquímica)

As 2 últimas lâminas foram submetidas ao método de imunohistoquímica, através da utilização de anticorpos comerciais primários específicos para cada proteína do estudo, seguindo os diferentes tipos de cadeia pesada de miosina Fast e Slow. Os cortes foram fixados com acetona gelada, lavados e ocorreu o bloqueio da peroxidade endógena com peróxido de hidrogênio (H2O2) 3% em metanol por 15 minutos. Seguiu-se 3 lavagens de 3 minutos em TBSt e o bloqueio de interações proteína-proteína não específicos por solução de albumina bovina a 2% em TBSt por 1 hora a 37ºC; as lâminas então foram incubadas com anticorpo primário (Tabela 1), diluído em solução de albumina bovina a 1%, em câmara úmida por 60 minutos. Após 3 lavagens de 3 minutos com tampão TBSt, foi realizada incubação com H-Histofine (Multi - Nichirei), o qual atua como anticorpo secundário, em câmara úmida por 30 minutos. Seguiram 3 lavagens de 3 minutos com TBSt. A revelação foi realizada com solução de substrato cromogênico DAB (1:50), em banho de 5 minutos em câmara escura, a contra-coloração foi realizada utilizando Hematoxilina de Harris. A frequência dos tipos de fibras foi realizada no “Image J” (Schneider *et*

al., 2012), sendo utilizadas em torno de 200 fibras musculares selecionadas a partir de 3-4 campos aleatórios.

Tabela 1. Relação dos anticorpos primários para a técnica de Imunohistoquímica

Anticorpo monoclonal	Empresa	Diluição
Primário:Anti-miosina rápida	Novocastra (MYHCf)	1:130
Secundário: Anti-miosina lenta	Novocastra (MYHCs)	1:180

2.5 Análise das JNMs e das fibras musculares em microscopia de luz e eletrônica de transmissão

A partir do terço médio dos músculos sóleos fixados em solução de Karnovsky (glutaraldeído a 2% e paraformoldeído a 4,0% em tampão fosfato de sódio 0,1M, ph 7,4). A seguir os mesmos foram para as seguintes análises:

2.5.1 Análise morfológica e morfométrica das JNMs através de microscopia de luz (Esterase Inespecífica) (n=5)

Através do uso de uma gilete, foram realizadas 2 secções longitudinais as quais foram submetidas à reação de Esterase Inespecífica (Lehrer e Ornstein, 1959), para caracterização das JNM. As peças foram lavadas durante 1 minuto em tampão fosfato 0,1M pH 7,4, incubadas a 37°C durante 5-10 minutos, no seguinte meio (pH 6,8-7,2): solução Tris HCl –20ml (Tris aminometano 6,05g + ácido clorídrico concentrado 3,34ml + água destilada 100ml), alfa naftil acetato a 1% - 0,5 ml (alfa naftil 1,0g + acetona 100ml) e pararosanilina azotizada – 1,6ml (pararosanilina 0,8ml + nitrito de sódio a 4% 0,8ml). A solução estoque de pararosanilina consistiu em 1,0ml de pararosanilina, 20 ml de água destilada e 5 ml de ácido clorídrico que, após a preparação, foi aquecida, resfriada e filtrada. Após a incubação no meio descrito acima, as peças foram lavadas em água corrente por 5 minutos, desidratadas, diafanizadas e montadas em lâminas para o estudo morfológico e morfométrico das JNMs. As lâminas preparadas para o estudo da

morfologia das junções neuromusculares foram também utilizadas para a análise morfométrica. A fotomicrografia das JNMs foi realizada em analisador de imagens Olympus Bx41(câmera SC30) do Departamento de Anatomia/IBB. Para cada animal estudado, foram tomadas medidas da área de 50 junções. As medidas foram analisadas com auxílio do software livre “ImageJ” (Schneider *et al.*, 2012).

2.5.2 Análise ultraestrutural das fibras musculares do músculo sóleo e das JNMs associadas (n=3)

Em 3 animais de cada grupo os músculos sóleos direitos foram reduzidos ao terço médio contendo o ponto motor. Foram obtidos fragmentos retangulares do músculo sóleo das áreas seccionadas a fim de se obterem secções longitudinais das fibras musculares e junções associadas. Imediatamente após sua redução, os fragmentos musculares foram mantidos em solução de Karnovsky e seguiram a rotina do Centro de Microscopia Eletrônica/IBB (CME/IBB). Através de cortes semi-finos corados em mistura de azul de metileno 1% e azul II 1% em solução de bórax 1%, os campos foram selecionados e a partir dos mesmos, foram realizados cortes ultrafinos através de ultramicrótomo Ultratome III 880 da LKB. Os cortes ultrafinos foram corados com solução de acetato de uracila em álcool 50% e, posteriormente, em citrato de chumbo. O material, então, foi visualizado e fotografado em Microscópio Eletrônico de Transmissão (TECNAI Spirit Fei Company) do CME/IBB.

2.6 Quantificação proteica (Western Blot) do PCNA (proliferação celular) e PAX7 (células satélites) (n=5)

Amostras das porções distais dos músculos sóleos de cada grupo experimental foram utilizadas. As amostras de tecido foram homogeneizadas em RIPA e inibidores de proteases (30mg de tecido/100µl de tampão de extração). Os extratos dos tecidos foram obtidos por centrifugação durante 10 minutos a 14000 rpm a 4ºC. O conteúdo de proteína foi determinado pelo método de Bradford (Bio-Rad protein assay) e o correspondente a 75 microgramas de proteínas foi aplicado no gel de poliacrilamida. Após eletroforese, o material foi transferido para membranas de nitrocelulose seguindo-se o bloqueio com leite

desnatado a 3% em TBS-T, e então incubadas com os anticorpos primário específicos (tabela 2), overnight a 4ºC. As membranas foram em seguida lavadas com TBSt e posteriormente foram incubadas por 1 hora em anticorpo secundário específico e reveladas utilizando-se substrato quimioluminescente para Western blotting (AMERSHAM ECLTM PRIME, GE Healthcare). A análise semiquantitativa de densitometria das bandas foi realizada pelo software “Image J” (Schneider *et al.*, 2012). Os dados foram normalizados com GAPDH.

Tabela 2. Relação dos anticorpos primários para a técnica de Western Blotting.

Proteína	Anticorpo Primário	Fabricante	Código
Pax7	Pax7	Abcam	ab -199010
PCNA	PCNA	Abcam	ab – 29
GAPDH	GAPDH	Cell Signaling	#2118

2.9 Análise estatística

Os resultados foram expressos em média e desvio padrão, sendo que foram consideradas diferenças estatisticamente significativas quando $p < 0,05$. Para as análises de Amplitude e Latência, área e diâmetro dos axônios e fibras nervosas, espessura da bainha de mielina, razão G, peso dos músculos sóleo, porcentagem de colágeno, quantificação proteica de Pax7 e PCNA e área das fibras musculares e JNMs foi utilizada técnica para análise de variância para o modelo com um fator complementado com teste de comparações múltiplas de Tukey (Zar, 2009). Para as análises do peso dos animais e da razão do tempo de contato foi utilizada técnica para análise de variância para o modelo de medidas repetidas em grupos independentes complementado com teste de comparações múltiplas de Bonferroni (Johnson e Wichern, 2014). Para o número de axônios e fibras nervosas foi utilizada técnica para análise de variância não paramétrica (Kruskal-Wallis) para o modelo com um fator complementado com teste de comparações múltiplas de Dunn (Zar, 2009). Para razão da área da pegada, razão da área de máximo contato e índice Funcional do Fibular foi utilizada, técnica para análise de variância não paramétrica para o modelo de medidas repetidas em grupos independentes complementado com teste de comparações múltiplas de Dunn (Johnson e Wichern, 2014).

Referências Bibliográficas

ALLUIN, O. et al. Functional recovery after peripheral nerve injury and implantation of a collagen guide. **Biomaterials,** v. 30, n. 3, p. 363-73, Jan 2009. ISSN 1878-5905 (Electronic) 0142-9612 (Linking). Disponível em: < http://www.ncbi.nlm.nih.gov/pubmed/18929405 >.

ANZIL, A. P.; WERNIG, A. Muscle fibre loss and reinnervation after long-term denervation. **J Neurocytol,** v. 18, n. 6, p. 833-45, Dec 1989. ISSN 0300-4864 (Print) 0300-4864 (Linking). Disponível em: < http://www.ncbi.nlm.nih.gov/pubmed/2621479 >.

ASPLUND, M. et al. Incidence of traumatic peripheral nerve injuries and amputations in Sweden between 1998 and 2006. **Neuroepidemiology,** v. 32, n. 3, p. 217-28, 2009. ISSN 1423-0208 (Electronic) 0251-5350 (Linking). Disponível em: < http://www.ncbi.nlm.nih.gov/pubmed/19174611 >.

BAIN, J.; MACKINNON, S.; HUNTER, D. Functional evaluation of complete sciatic, peroneal, and posterior tibial nerve lesions in the rat. **Plastic and reconstructive surgery,** v. 83, n. 1, p. 129-136, 1989. ISSN 0032-1052.

BARROS, L. C. et al. A new fibrin sealant from Crotalus durissus terrificus venom: applications in medicine. **J Toxicol Environ Health B Crit Rev,** v. 12, n. 8, p. 553-71, Oct 2009. ISSN 1521-6950 (Electronic) 1093-7404 (Linking). Disponível em: < http://www.ncbi.nlm.nih.gov/pubmed/20183534 >.

BENTOLILA, V. et al. Complete traumatic brachial plexus palsy. Treatment and outcome after repair. **J Bone Joint Surg Am,** v. 81, n. 1, p. 20-8, Jan 1999. ISSN 0021-9355 (Print) 0021-9355 (Linking). Disponível em: < http://www.ncbi.nlm.nih.gov/pubmed/9973050 >.

BISCOLA, N. P. et al. Multiple uses of fibrin sealant for nervous system treatment following injury and disease. **J Venom Anim Toxins Incl Trop Dis,** v. 23, p. 13, 2017. ISSN 1678-9199 (Print) 1678-9180 (Linking). Disponível em: < http://www.ncbi.nlm.nih.gov/pubmed/28293254 >.

BONNEMANN, C.; BUSHBY, K. The limb-girdle muscular dystrophies. **Engel AG; Franzini Armstrong A, editors Myology 3rd McGraw-Hill**, p. 1077-1121, 2004.

BORISOV, A. B.; CARLSON, B. M. Cell death in denervated skeletal muscle is distinct from classical apoptosis. **Anat Rec,** v. 258, n. 3, p. 305-18, Mar 01 2000. ISSN 0003-276X (Print) 0003-276X (Linking). Disponível em: < http://www.ncbi.nlm.nih.gov/pubmed/10705351 >.

BORISOV, A. B.; DEDKOV, E. I.; CARLSON, B. M. Abortive myogenesis in denervated skeletal muscle: differentiative properties of satellite cells, their migration, and block of terminal differentiation. **Anatomy and embryology,** v. 209, n. 4, p. 269-279, 2005. ISSN 0340-2061.

BUCHAIM, R. L. et al. Effect of low-level laser therapy (LLLT) on peripheral nerve regeneration using fibrin glue derived from snake venom. **Injury,** v. 46, n. 4, p. 655-60, Apr 2015. ISSN 1879-0267 (Electronic) 0020-1383 (Linking). Disponível em: < http://www.ncbi.nlm.nih.gov/pubmed/25669962 >.

BURNETT, M. G.; ZAGER, E. L. Pathophysiology of peripheral nerve injury: a brief review. **Neurosurg Focus,** v. 16, n. 5, p. E1, May 15 2004. ISSN 1092-0684 (Electronic)
1092-0684 (Linking). Disponível em: < http://www.ncbi.nlm.nih.gov/pubmed/15174821 >.

CARTAROZZI, L. P. et al. Mesenchymal stem cells engrafted in a fibrin scaffold stimulate Schwann cell reactivity and axonal regeneration following sciatic nerve tubulization. **Brain research bulletin,** v. 112, p. 14-24, 2015. ISSN 0361-9230.

CHARGE, S. B.; RUDNICKI, M. A. Cellular and molecular regulation of muscle regeneration. **Physiol Rev,** v. 84, n. 1, p. 209-38, Jan 2004. ISSN 0031-9333 (Print)
0031-9333 (Linking). Disponível em: < http://www.ncbi.nlm.nih.gov/pubmed/14715915 >.

CHIMUTENGWENDE-GORDON, M.; KHAN, W. Recent advances and developments in neural repair and regeneration for hand surgery. **Open Orthop J,** v. 6, p. 103-7, 2012. ISSN 1874-3250 (Electronic)
1874-3250 (Linking). Disponível em: < http://www.ncbi.nlm.nih.gov/pubmed/22431954 >.

CONFORTIM, H. D. et al. Effects of aging and maternal protein restriction on the muscle fibers morphology and neuromuscular junctions of rats after nutritional recovery. **Micron,** v. 71, p. 7-13, 2015. ISSN 0968-4328.

COULET, B. et al. A comparison of intercostal and partial ulnar nerve transfers in restoring elbow flexion following upper brachial plexus injury (C5-C6±C7). **The Journal of hand surgery,** v. 35, n. 8, p. 1297-1303, 2010. ISSN 0363-5023.

DE OLIVEIRA GONÇALVES, J. B. et al. Effects of low-level laser therapy on autogenous bone graft stabilized with a new heterologous fibrin sealant. **Journal of Photochemistry and Photobiology B: Biology,** v. 162, p. 663-668, 2016. ISSN 1011-1344.

ENGEL, A.; ORAWA, E. Chapter 34: Dystrophinopathies. **Myology,(Aggiungere: McGraw-Hill),** v. 978, 2004.

ENGEL, A. G. Chapter 3 The neuromuscular junction. In: (Ed.). **Handbook of Clinical Neurology**: Elsevier, v.Volume 91, 2008. p.103-148. ISBN 0072-9752.

FARRAG, T. Y. et al. Effect of platelet rich plasma and fibrin sealant on facial nerve regeneration in a rat model. **Laryngoscope,** v. 117, n. 1, p. 157-65, Jan 2007. ISSN 0023-852X (Print)
0023-852X (Linking). Disponível em: < http://www.ncbi.nlm.nih.gov/pubmed/17202946 >.

FELIX, S. P. et al. Comparison between suture and fibrin glue on repair by direct coaptation or tubulization of injured mouse sciatic nerve. **Microsurgery,** v. 33, n. 6, p. 468-77, Sep 2013. ISSN 1098-2752 (Electronic)
0738-1085 (Linking). Disponível em: < http://www.ncbi.nlm.nih.gov/pubmed/23836677 >.

FERREIRA, A. S. **Lesões Nervosas Periféricas - Diagnóstico E Tratamento**. 2a./2001. 2001. ISBN 8572881964.

FERREIRA, R. S. Autologous or heterologous fibrin sealant scaffold: which is the better choice? **Journal of Venomous Animals and Toxins Including Tropical Diseases,** v. 20, n. 1, p. 31, 2014. ISSN 1678-9199.

FITTON, A.; BERRY, M.; MCGREGOR, A. Preservation of denervated muscle form and function by clenbuterol in a rat model of peripheral nerve injury. **Journal of Hand Surgery,** v. 26, n. 4, p. 335-346, 2001. ISSN 0266-7681.

FRANK, E.; GAUTVIK, K.; SOMMERSCHILD, H. Cholinergic receptors at denervated mammalian motor end-plates. **Acta Physiol Scand,** v. 95, n. 1, p. 66-76, Sep 1975. ISSN 0001-6772 (Print)
0001-6772 (Linking). Disponível em: < http://www.ncbi.nlm.nih.gov/pubmed/1180105 >.

FROST, H. K. et al. G-CSF prevents caspase 3 activation in Schwann cells after sciatic nerve transection, but does not improve nerve regeneration. **Neuroscience,** v. 334, p. 55-63, 2016. ISSN 0306-4522.

FU, S. Y.; GORDON, T. Contributing factors to poor functional recovery after delayed nerve repair: prolonged denervation. **J Neurosci,** v. 15, n. 5 Pt 2, p. 3886-95, May 1995. ISSN 0270-6474 (Print)
0270-6474 (Linking). Disponível em: < http://www.ncbi.nlm.nih.gov/pubmed/7751953 >.

GASPAROTTO, V. P. et al. A new fibrin sealant as a three-dimensional scaffold candidate for mesenchymal stem cells. **Stem Cell Res Ther,** v. 5, n. 3, p. 78, Jun 10 2014. ISSN 1757-6512 (Electronic)
1757-6512 (Linking). Disponível em: < http://www.ncbi.nlm.nih.gov/pubmed/24916098 >.

GASPAROTTO, V. P. et al. A new fibrin sealant as a three-dimensional scaffold candidate for mesenchymal stem cells. **Stem cell research & therapy,** v. 5, n. 3, p. 78, 2014. ISSN 1757-6512.

GATTI, M. et al. Treatment of venous ulcers with fibrin sealant derived from snake venom. **Journal of Venomous Animals and Toxins including Tropical Diseases,** v. 17, n. 2, p. 226-229, 2011. ISSN 1678-9199.

GAUDET, A. D.; POPOVICH, P. G.; RAMER, M. S. Wallerian degeneration: gaining perspective on inflammatory events after peripheral nerve injury. **J Neuroinflammation,** v. 8, p. 110, Aug 30 2011. ISSN 1742-2094 (Electronic)
1742-2094 (Linking). Disponível em: < http://www.ncbi.nlm.nih.gov/pubmed/21878126 >.

GENSEL, J. C. et al. Behavioral and histological characterization of unilateral cervical spinal cord contusion injury in rats. **Journal of neurotrauma,** v. 23, n. 1, p. 36-54, 2006. ISSN 0897-7151.

GERMINARIO, E. et al. Early changes of type 2B fibers after denervation of rat EDL skeletal muscle. **Journal of Applied Physiology,** v. 92, n. 5, p. 2045-2052, 2002. ISSN 8750-7587.

GIORDANI, G. et al. Tratamento da paralisia facial por neurotização. **Arq Catarinenses Med,** v. 38, p. 152-154, 2009.

GORDON, T. Nerve Regeneration: Understanding Biology and Its Influence on Return of Function After Nerve Transfers. **Hand Clin,** v. 32, n. 2, p. 103-17, May 2016. ISSN 1558-1969 (Electronic)
0749-0712 (Linking). Disponível em: < http://www.ncbi.nlm.nih.gov/pubmed/27094884 >.

GORDON, T.; HEGEDUS, J.; TAM, S. L. Adaptive and maladaptive motor axonal sprouting in aging and motoneuron disease. **Neurological research,** v. 26, n. 2, p. 174-185, 2004. ISSN 0161-6412.

GRIFFIN, J. W. et al. Peripheral nerve repair and reconstruction. **JBJS,** v. 95, n. 23, p. 2144-2151, 2013. ISSN 0021-9355.

GRINSELL, D.; KEATING, C. P. Peripheral nerve reconstruction after injury: a review of clinical and experimental therapies. **Biomed Res Int,** v. 2014, p. 698256, 2014. ISSN 2314-6141 (Electronic). Disponível em: < http://www.ncbi.nlm.nih.gov/pubmed/25276813 >.

GUTMANN, E. Effect of delay of innervation on recovery of muscle after nerve lesions. **Journal of neurophysiology,** v. 11, n. 4, p. 279-294, 1948. ISSN 0022-3077.

GUTMANN, E.; ZELENA, J. Morphological changes in the denervated muscle. In: (Ed.). **The denervated muscle**: Springer, 1962. p.57-102.

HARTZELL, H. C.; FAMBROUGH, D. M. Acetylcholine receptors. Distribution and extrajunctional density in rat diaphragm after denervation correlated with acetylcholine sensitivity. **J Gen Physiol,** v. 60, n. 3, p. 248-62, Sep 1972. ISSN 0022-1295 (Print)
0022-1295 (Linking). Disponível em: < http://www.ncbi.nlm.nih.gov/pubmed/5055788 >.

HIGASHINO, K. et al. Early changes in muscle atrophy and muscle fiber type conversion after spinal cord transection and peripheral nerve transection in rats. **Journal of neuroengineering and rehabilitation,** v. 10, n. 1, p. 46, 2013. ISSN 1743-0003.

ISAACS, J. E. et al. Comparative analysis of biomechanical performance of available “nerve glues”. **The Journal of hand surgery,** v. 33, n. 6, p. 893-899, 2008. ISSN 0363-5023.

JOHNSON, R. A.; WICHERN, D. W. **Applied multivariate statistical analysis**. Prentice-Hall New Jersey, 2014.

JUDSON, R. N.; ZHANG, R. H.; ROSSI, F. Tissue-resident mesenchymal stem/progenitor cells in skeletal muscle: collaborators or saboteurs? **The FEBS journal,** v. 280, n. 17, p. 4100-4108, 2013. ISSN 1742-4658.

KANG, J. R.; ZAMORANO, D. P.; GUPTA, R. Limb salvage with major nerve injury: current management and future directions. **J Am Acad Orthop Surg,** v. 19 Suppl 1, p. S28-34, 2011. ISSN 1067-151X (Print)
1067-151X (Linking). Disponível em: < http://www.ncbi.nlm.nih.gov/pubmed/21304044 >.

KIM, D. H. et al. Outcomes of surgery in 1019 brachial plexus lesions treated at Louisiana State University Health Sciences Center. **J Neurosurg,** v. 98, n. 5, p. 1005-16, May 2003. ISSN 0022-3085 (Print)

0022-3085 (Linking). Disponível em: < http://www.ncbi.nlm.nih.gov/pubmed/12744360 >.

KURIMOTO, S. et al. Activation of the Wnt/β-catenin signaling cascade after traumatic nerve injury. **Neuroscience,** v. 294, p. 101-108, 2015. ISSN 0306-4522.

LEHRER, G. M.; ORNSTEIN, L. A diazo coupling method for the electron microscopic localization of cholinesterase. **The Journal of Cell Biology,** v. 6, n. 3, p. 399-406, 1959. ISSN 0021-9525.

LIN, S. et al. The role of nerve- versus muscle-derived factors in mammalian neuromuscular junction formation. **J Neurosci,** v. 28, n. 13, p. 3333-40, Mar 26 2008. ISSN 1529-2401 (Electronic)
0270-6474 (Linking). Disponível em: < http://www.ncbi.nlm.nih.gov/pubmed/18367600 >.

LIU, H.-F. et al. Can the Babysitter Procedure Improve Nerve Regeneration and Denervated Muscle Atrophy in the Treatment of Peripheral Nerve Injury? **Plastic and reconstructive surgery,** v. 138, n. 1, p. 122-131, 2016. ISSN 0032-1052.

LOPES, C. D. et al. BDNF gene delivery mediated by neuron-targeted nanoparticles is neuroprotective in peripheral nerve injury. **Biomaterials,** v. 121, p. 83-96, 2017. ISSN 0142-9612.

LOUGHNA, P.; MORGAN, M. Passive stretch modulates denervation induced alterations in skeletal muscle myosin heavy chain mRNA levels. **Pflügers Archiv European Journal of Physiology,** v. 439, n. 1, p. 52-55, 1999. ISSN 0031-6768.

LUNDBORG, G. Nerve regenration and repair: A review. **Acta Orthopaedica Scandinavica,** v. 58, n. 2, p. 145-169, 1987. ISSN 0001-6470.

LUNDBORG, G. A 25-year perspective of peripheral nerve surgery: evolving neuroscientific concepts and clinical significance. **The Journal of hand surgery,** v. 25, n. 3, p. 391-414, 2000. ISSN 0363-5023.

MA, J. et al. Gene expression of myogenic regulatory factors, nicotinic acetylcholine receptor subunits, and GAP-43 in skeletal muscle following denervation in a rat model. **J Orthop Res,** v. 25, n. 11, p. 1498-505, Nov 2007. ISSN 0736-0266 (Print)
0736-0266 (Linking). Disponível em: < http://www.ncbi.nlm.nih.gov/pubmed/17568415 >.

MACIEL, F. O. et al. Effect of electrical stimulation of the cranial tibial muscle after end-to-side neurorrhaphy of the peroneal nerve in rats. **Acta Cir Bras,** v. 28, n. 1, p. 39-47, Jan 2013. ISSN 1678-2674 (Electronic)
0102-8650 (Linking). Disponível em: < http://www.ncbi.nlm.nih.gov/pubmed/23338112 >.

MALOMOUZH, A. I. Non-cholinergic signaling pathways at vertebrate neuromuscular junctions. In: (Ed.). **Skeletal Muscle-From Myogenesis to Clinical Relations**: InTech, 2012.

MARTINS, R. S. et al. Electrophysiologic assessment of regeneration in rat sciatic nerve repair using suture, fibrin glue or a combination of both techniques. **Arq Neuropsiquiatr,** v. 63, n. 3A, p. 601-4, Sep 2005. ISSN 0004-282X (Print)
0004-282X (Linking). Disponível em: < http://www.ncbi.nlm.nih.gov/pubmed/16172708 >.

MENDONÇA, A. C.; BARBIERI, C. H.; MAZZER, N. Directly applied low intensity direct electric current enhances peripheral nerve regeneration in rats. **Journal of neuroscience methods,** v. 129, n. 2, p. 183-190, 2003. ISSN 0165-0270.

MICHAEL, F. et al. Denervation-induced mitochondrial dysfunction and autophagy in skeletal muscle of apoptosis-deficient animals. **American Journal of Physiology-Cell Physiology,** v. 303, n. 4, p. C447-C454, 2012. ISSN 0363-6143.

MOIMAS, S. et al. Effect of vascular endothelial growth factor gene therapy on post-traumatic peripheral nerve regeneration and denervation-related muscle atrophy. **Gene Ther,** v. 20, n. 10, p. 1014-21, Oct 2013. ISSN 1476-5462 (Electronic)
0969-7128 (Linking). Disponível em: < http://www.ncbi.nlm.nih.gov/pubmed/23719064 >.

NAKAMURA, T. et al. Experimental study on the regeneration of peripheral nerve gaps through a polyglycolic acid-collagen (PGA-collagen) tube. **Brain Res,** v. 1027, n. 1-2, p. 18-29, Nov 19 2004. ISSN 0006-8993 (Print)
0006-8993 (Linking). Disponível em: < http://www.ncbi.nlm.nih.gov/pubmed/15494153 >.

NGUYEN, Q. T.; SANES, J. R.; LICHTMAN, J. W. Pre-existing pathways promote precise projection patterns. **Nat Neurosci,** v. 5, n. 9, p. 861-7, Sep 2002. ISSN 1097-6256 (Print)
1097-6256 (Linking). Disponível em: < https://www.ncbi.nlm.nih.gov/pubmed/12172551 >.

NIKOLAOU, S. et al. Contribution of denervated muscle to contractures after neonatal brachial plexus injury: not just muscle fibrosis. **Muscle & nerve,** v. 49, n. 3, p. 398-404, 2014. ISSN 1097-4598.

NISHIMURA, M. T. et al. Mechanical resistance of peripheral nerve repair with biological glue and with conventional suture at different postoperative times. **J Reconstr Microsurg,** v. 24, n. 5, p. 327-32, Jul 2008. ISSN 0743-684X (Print)
0743-684X (Linking). Disponível em: < http://www.ncbi.nlm.nih.gov/pubmed/18597220 >.

OHIRA, T. et al. The effects of heat stress on morphological properties and intracellular signaling of denervated and intact soleus muscles in rats. **Physiological reports,** v. 5, n. 15, p. e13350, 2017. ISSN 2051-817X.

PATTERSON, M. F.; STEPHENSON, G.; STEPHENSON, D. G. Denervation produces different single fiber phenotypes in fast-and slow-twitch hindlimb muscles of the rat. **American Journal of Physiology-Cell Physiology,** v. 291, n. 3, p. 518-528, 2006. ISSN 0363-6143.

PERUSSI BISCOLA, N. et al. Long-standing motor and sensory recovery following acute fibrin sealant based neonatal sciatic nerve repair. **Neural plasticity,** v. 2016, 2016. ISSN 2090-5904.

PETTE, D.; VRBOVA, G. Neural control of phenotypic expression in mammalian muscle fibers. **Muscle Nerve,** v. 8, n. 8, p. 676-89, Oct 1985. ISSN 0148-639X (Print)
0148-639X (Linking). Disponível em: < http://www.ncbi.nlm.nih.gov/pubmed/3903491 >.

PINHEIRO-DARDIS, C. M.; RUSSO, T. L. Electrical stimulation based on chronaxie increases fibrosis and modulates TWEAK/Fn14, TGF-β/myostatin, and MMP pathways in denervated muscles. **American journal of physical medicine & rehabilitation,** v. 96, n. 4, p. 260-267, 2017. ISSN 0894-9115.

RAFIJAH, G. et al. The effects of adjuvant fibrin sealant on the surgical repair of segmental nerve defects in an animal model. **J Hand Surg Am,** v. 38, n. 5, p. 847-55, May 2013. ISSN 1531-6564 (Electronic)
0363-5023 (Linking). Disponível em: < http://www.ncbi.nlm.nih.gov/pubmed/23561728 >.

RAY, W. Z.; MACKINNON, S. E. Management of nerve gaps: autografts, allografts, nerve transfers, and end-to-side neurorrhaphy. **Exp Neurol,** v. 223, n. 1, p. 77-85, May 2010. ISSN 1090-2430 (Electronic)
0014-4886 (Linking). Disponível em: < http://www.ncbi.nlm.nih.gov/pubmed/19348799 >.

RICH, M. M.; LICHTMAN, J. W. In vivo visualization of pre- and postsynaptic changes during synapse elimination in reinnervated mouse muscle. **J Neurosci,** v. 9, n. 5, p. 1781-805, May 1989. ISSN 0270-6474 (Print)
0270-6474 (Linking). Disponível em: < https://www.ncbi.nlm.nih.gov/pubmed/2542480 >.

ROBINSON, L. R. Traumatic injury to peripheral nerves. **Muscle Nerve,** v. 23, n. 6, p. 863-73, Jun 2000. ISSN 0148-639X (Print)
0148-639X (Linking). Disponível em: < http://www.ncbi.nlm.nih.gov/pubmed/10842261 >.

RODRIGUES, A. D. C.; SILVA, M. D. P. Inside-out versus standard artery graft to repair a sensory nerve in rats. **Microsurgery,** v. 21, n. 3, p. 102-107, 2001. ISSN 1098-2752.

RUVEN, C. et al. Transplantation of Embryonic Spinal Cord Derived Cells Helps to Prevent Muscle Atrophy after Peripheral Nerve Injury. **International journal of molecular sciences,** v. 18, n. 3, p. 511, 2017.

RUVEN, C.; WU, W. Transplantation of embryonic spinal cord derived cells to prevent muscle atrophy after various peripheral nerve injuries. 2017 Hong Kong Inter-University Postgraduate Symposium in Biochemical Sciences, 2017.

SAKAKIMA, H. et al. Effects of short-term denervation and subsequent reinnervation on motor endplates and the soleus muscle in the rat. **Archives of histology and cytology,** v. 63, n. 5, p. 495-506, 2000. ISSN 0914-9465.

SAKUMA, M. et al. Lack of motor recovery after prolonged denervation of the neuromuscular junction is not due to regenerative failure. **Eur J Neurosci,** v. 43, n. 3, p. 451-62, Feb 2016. ISSN 1460-9568 (Electronic)
0953-816X (Linking). Disponível em: < http://www.ncbi.nlm.nih.gov/pubmed/26332731 >.

SCHMALBRUCH, H.; LEWIS, D. M. Dynamics of nuclei of muscle fibers and connective tissue cells in normal and denervated rat muscles. **Muscle Nerve,** v. 23, n. 4, p. 617-26, Apr 2000. ISSN 0148-639X (Print)
0148-639X (Linking). Disponível em: < http://www.ncbi.nlm.nih.gov/pubmed/10716774 >.

SCHNEIDER, C. A.; RASBAND, W. S.; ELICEIRI, K. W. NIH Image to ImageJ: 25 years of image analysis. **Nature methods,** v. 9, n. 7, p. 671-675, 2012. ISSN 1548-7091.

SEDDON, H. A classification of nerve injuries. **British medical journal,** v. 2, n. 4260, p. 237, 1942.

SEDDON, H. J. A Classification of Nerve Injuries. **Br Med J,** v. 2, n. 4260, p. 237-9, Aug 29 1942. ISSN 0007-1447 (Print)
0007-1447 (Linking). Disponível em: < http://www.ncbi.nlm.nih.gov/pubmed/20784403 >.

SIEMIONOW, M.; SONMEZ, E. Nerve allograft transplantation: a review. **J Reconstr Microsurg,** v. 23, n. 8, p. 511-20, Nov 2007. ISSN 0743-684X (Print)
0743-684X (Linking). Disponível em: < http://www.ncbi.nlm.nih.gov/pubmed/18189213 >.

SOBRAL, L. et al. Immediate versus later exercises for rat sciatic nerve regeneration after axonotmesis: histomorphometric and functional analyses. **Brazilian Journal of Physical Therapy,** v. 12, n. 4, p. 311-316, 2008. ISSN 1413-3555.

STEINBACH, J. H. Neuromuscular junctions and alpha-bungarotoxin-binding sites in denervated and contralateral cat skeletal muscles. **J Physiol,** v. 313, p. 513-28, 1981. ISSN 0022-3751 (Print)
0022-3751 (Linking). Disponível em: < http://www.ncbi.nlm.nih.gov/pubmed/7277234 >.

SU, Z. et al. Acupuncture plus low-frequency electrical stimulation (Acu-LFES) attenuates denervation-induced muscle atrophy. **Journal of Applied Physiology,** v. 120, n. 4, p. 426-436, 2016. ISSN 8750-7587.

SULLIVAN, R. et al. Peripheral Nerve Injury: Stem Cell Therapy and Peripheral Nerve Transfer. **Int J Mol Sci,** v. 17, n. 12, Dec 14 2016. ISSN 1422-0067 (Electronic)
1422-0067 (Linking). Disponível em: < http://www.ncbi.nlm.nih.gov/pubmed/27983642 >.

TEMPLE, C. L. et al. Resistance to disruption and gapping of peripheral nerve repairs: an in vitro biomechanical assessment of techniques. **J Reconstr Microsurg,** v. 20, n. 8, p. 645-50, Nov 2004. ISSN 0743-684X (Print)
0743-684X (Linking). Disponível em: < http://www.ncbi.nlm.nih.gov/pubmed/15630661 >.

TINTIGNAC, L. A.; BRENNER, H. R.; RUEGG, M. A. Mechanisms Regulating Neuromuscular Junction Development and Function and Causes of Muscle Wasting. **Physiol Rev,** v. 95, n. 3, p. 809-52, Jul 2015. ISSN 1522-1210 (Electronic)
0031-9333 (Linking). Disponível em: < http://www.ncbi.nlm.nih.gov/pubmed/26109340 >.

TRICAUD, N.; PARK, H. T. Wallerian demyelination: chronicle of a cellular cataclysm. **Cellular and Molecular Life Sciences**, p. 1-9, 2017. ISSN 1420-682X.

TU, H. et al. Morphological Regeneration and Functional Recovery of Neuromuscular Junctions after Tourniquet-Induced Injuries in Mouse Hindlimb. **Front Physiol,** v. 8, p. 207, 2017. ISSN 1664-042X (Print)
1664-042X (Linking). Disponível em: < http://www.ncbi.nlm.nih.gov/pubmed/28428759 >.

TUFFAHA, S. H. et al. Growth hormone therapy accelerates axonal regeneration, promotes motor reinnervation, and reduces muscle atrophy following peripheral nerve injury. **Plastic and reconstructive surgery,** v. 137, n. 6, p. 1771-1780, 2016. ISSN 0032-1052.

UYANIKGIL, Y. et al. Useful Effects of Melatonin in Peripheral Nerve Injury and Development of the Nervous System. **J Brachial Plex Peripher Nerve Inj,** v. 12, n. 1, p. e1-e6, Jan 2017. ISSN 1749-7221 (Print)
1749-7221 (Linking). Disponível em: < http://www.ncbi.nlm.nih.gov/pubmed/28603548 >.

VICENTE, E. J. D. et al. Recuperação funcional do nervo ciático reparado pela cola de fibrina. **HU Revista,** v. 34, n. 1, p. 9-12, 2008. ISSN 0103-3123.

VITERBO, F. et al. Latero-terminal neurorrhaphy without removal of the epineural sheath. Experimental study in rats. **Revista paulista de medicina,** v. 110, n. 6, p. 267-275, 1992. ISSN 0035-0362.

WIBERG, R. et al. Investigation of the expression of myogenic transcription factors, microRNAs and muscle-specific E3 ubiquitin ligases in the medial gastrocnemius and soleus muscles following peripheral nerve injury. **PloS one,** v. 10, n. 12, p. e0142699, 2015. ISSN 1932-6203.

WILLAND, M. P. et al. Daily electrical muscle stimulation enhances functional recovery following nerve transection and repair in rats. **Neurorehabilitation and neural repair,** v. 29, n. 7, p. 690-700, 2015. ISSN 1545-9683.

WINDISCH, A. et al. Fast to slow transformation of denervated and electrically stimulated rat muscle. **J Physiol,** v. 510 (Pt 2), p. 623-32, Jul 15 1998. ISSN 0022-3751 (Print)
0022-3751 (Linking). Disponível em: < http://www.ncbi.nlm.nih.gov/pubmed/9706009 >.

WU, P. et al. Key changes in denervated muscles and their impact on regeneration and reinnervation. **Neural regeneration research,** v. 9, n. 20, p. 1796, 2014.

XING, H. et al. Electrical stimulation influences satellite cell differentiation after sciatic nerve crush injury in rats. **Muscle & nerve,** v. 51, n. 3, p. 400-411, 2015. ISSN 1097-4598.

ZAR, J. Biostatistical Analysis, 4th Impression, Dorling Kindersley (India) Pvt. **Ltd., Delhi,** v. 110, p. 92, 2009.

Capítulo 1

Heterologous fibrin sealant potentiates axonal regeneration after peripheral nerve injury with reduction in the number of suture points.

Ana Paula Silveira Leite [1,2], Arthur Alves Sartori [2], Felipe Cantore Tibúrcio[2], Carina Guidi Pinto[1,2], Benedito Barraviera[3], Rui Seabra Ferreira Junior[3], Antonio de Castro Rodrigues[4], André Luis Filadelpho[2], Selma Maria Matheus Michelin[2]*

[1] Graduate Program on the General Bases of Surgery, Botucatu Medical School, Department of Anatomy, Institute of Biosciences, UNESP - UNIV Estadual Paulista, Botucatu Campus, Travessa da Rua Prof. Dr. Gilberti Moreno, Zip Code: 18618-689, Botucatu, São Paulo, Brazil. E-mail: apsleitebio@hotmail.com

[2] Department of Anatomy, Institute of Biosciences, UNESP - UNIV Estadual Paulista, Botucatu Campus, Travessa da Rua Prof. Dr. Gilberti Moreno, Zip Code: 18618-689, Botucatu, São Paulo, Brazil.

[3] The Center for the Study of Venoms and Venomous Animals, UNESP, Botucatu, SP, Brazil

4 Unifai-Centro Universitário de Adamantina, Adamantina, SP, Brazil.

Corresponding author: Ana Paula Silveira Leite, Botucatu Medical School, Department of Anatomy, Institute of Biosciences, UNESP - UNIV Estadual Paulista, Botucatu Campus, Travessa da Rua Prof. Dr. Gilberti Moreno, Zip Code: 18618-689, Botucatu, São Paulo, Brazil. E-mail: apsleitebio@hotmail.com. Telephone: +55 (014) 3880-0025.

Este capítulo foi redigido de acordo com as normas de publicação da revista: **Experimental Neurology**, para a qual o mesmo será submetido.

Abstract

Muscle contraction requires the interaction between muscle and nerve to be intact. This interaction is determined by a specialized region, the neuromuscular junction (NMJ). The loss of connection between the axon and the muscle, due to peripheral nervous lesions, leads to degeneration of these structures, atrophy of the muscular fibers and fibrosis. In a scenario of complete transection of the nerve, surgical intervention is necessary for motor recovery. Among the different techniques used, the combined use of suture with fibrin glue has been highlighted with positive results. Among the existing sealants, the heterologous sealant developed by CEVAP (Center for the Study of Venoms and Venomous Animals) has important advantages, presenting no risk of transmission of infections, since it does not contain human blood in its composition. The purpose of this study was to evaluate the use of heterologous fibrin sealant (CEVAP) associated with reduced number of stitches (1 point) when compared with the use of conventional suture (3 stitches) after ischiatic nerve injury. Thirty-six adult male Wistar rats weredivided into four experimental groups: Control (C), Denervated (D); Suture (S) and Suture + Fibrin Sealant (SFS). In group C, only a superficial incision in the right antimer, separation from the musculature and location of the ischiatic nerve, was made. In group D, ischiatic nerve neurotmesis (6 mm gap) was performed. In group S, neurotmesis was carried out and after 7 days an epineural anastomosis was performed. In the SFS group, nerve reconstruction was performed with one suture point, followed by the application of the CEVAP fibrin sealant (Unesp - Botucatu Unesp Center for the Study of Poisons and Animals). Before performing the surgical procedures and on the 15th, 30th and 60th day after sectioning and burial of nerves, Catwalk analysis of all animals was performed according to the experimental groups. After the experimental period (the 60th day), animals were anesthetized for electromyography analysis and then euthanized. The ischiatic nerves, the muscle branches of the tibial nerve to the soleus muscle and the right-sided soleus muscles, were collected and subjected to: a) morphological (non-specific esterase) and morphometric analysis of NMJs by light and transmission microscopy; b) morphological and morphometric analysis of muscle fibers (HE); c) frequency of muscle fiber types (Fast and Slow); d) quantification of the percentage of collagen in muscle tissue; d) protein expression: PaX7 and PCNA (Western Blotting); e) morphological and morphometric analysis of the nerves (osmium tetroxide). Electromyography analysis revealed that the amplitude and latency values of the S and SFS groups were similar, indicating nerve regeneration. Catwalk analysis indicated that there was a functional deficit in all injury groups (D, S and SFS) at the end of the experimental period. The morphological analysis of the nerves revealed that the S and SFS groups approached the C, and the G ratio values remained within the normal range. In the ischiatic nerve, morphometric analysis showed superior values in the SFS group compared with the S group regarding the area and diameter of the axons and nerve fibers. In the S and SFS groups, there was an increase in muscle weight and a decrease in the percentage of collagen compared with group D. In the NMJs, the synaptic boutons were reestablished. There was an increase in the frequency of Fast fibers in the groups with lesion (D, S and SFS), and there was a type grouping pattern of distribution in them as well. Analysis of the protein expression of PaX7 and PCNA demonstrated similarity in the groups studied. The majority of results found in this study showed similarity between the S and SFS groups and a protective effect at the lesion site (ischiatic nerve) caused by the heterologous fibrin sealant use, was observed. Considering that the decrease in the number of stitches is able to reduce the trauma caused by the needle and it accelerates the surgical practice. So the heterologous fibrin sealant used in nerve reconstruction should be considered after peripheral nerve injury.

Keywords: peripheral nerve injury, heterologous fibrin sealant, neuromuscular interaction,neuromuscular junction,motor recovery.

1. Introduction

In vertebrates, skeletal striated muscle requires innervation of the motor nerve to produce skeletal muscle contractions and to avoid muscular atrophy (Tu *et al.*, 2017). The region of contact between motor neurons and their target muscle fibers is a morphologically distinct region called the neuromuscular junction (NMJ), which is responsible for electric signal transmission from the motor neuron to the mucle fibers, promoting muscle contraction. In order for muscular contraction to occur, structures that promote neuromuscular interaction must be intact (Malomouzh, 2012; Tintignac *et al.*, 2015).

Several factors may determine changes in NMJs, including peripheral nerve lesions (PNLs), which result in a loss of the connection between the axon and the muscle, leading to degeneration of these structures (Ruven e Wu, 2017).

PNLs constitute a common clinical scenario, and can lead to various complications and lifestyle impairments for the patients. These lesions affect approximately 13,9 individuals per 100 thousand, each year (Asplund *et al.*, 2009), and may lead to sensorial and or motor loss besides chronic pain (Sullivan *et al.*, 2016; Uyanikgil *et al.*, 2017).

When the injury occurs by complete transection of the nerve, with electrical conduction blockage, it is classified as neurotmese (Seddon, H. J., 1942). Following the injury, distally to the lesion occurs a disconnection of the axons and their cellular bodies, leading to muscle denervation. Axonal regeneration, although limited, occurs spontaneously in the peripheral nervous system. Functionally, axonal regeneration is the replacement of the injured distal nerve segment, allowing the reinnervation of the target organs and the reestablishment of their functions. Although there is a potential for spontaneous regeneration, functional recovery after nerve damage is limited in adults (Ray e Mackinnon, 2010).

The gold standard for reconstruction in this type of lesion is end-to-end neurorraphy (Rafijah *et al.*, 2013; Wu *et al.*, 2014), although the use of sutures may lead to inflammatory reactions including the formation of granuloma and neuroma and leading to chronic pain (Nakamura *et al.*, 2004; Chimutengwende-Gordon e Khan, 2012). An alternative to minimize the damage caused by suture use is to reduce the points used for reconstruction (Biscola *et al.*, 2017). In this regard, the

fibrine glue is a good strategy due to its adhesion capacity to tissues, and has been widely used in the medical field since the 70's (Isaacs *et al.*, 2008); however, there is an important disadvantage of the fibrine glue, since it contains blood-derived fibrinogen, potentially leading to adverse reactions (Nakamura *et al.*, 2004; Chimutengwende-Gordon e Khan, 2012).

The Center for the Study of Venoms and Venomous Animals (CEVAP-Unesp-Botucatu-SP) has developed a fibrin adhesive derived from the venom of the snake *Crotalus durissus terrificus* and is considered a biological and biodegradable heterologous sealant that does not produce adverse reactions. Because it is free of human blood, it is not a transmitter of infectious diseases, as well as having a good adhesive capacity, and is indicated for use along with traditional suture procedures (Barros *et al.*, 2009), its composition the cryoprecipitate containing fibrinogen and coagulation factors are derived from buffalo blood, and the functional thrombin is replaced by gyroxin, a thrombin-like protein also capable of cleaving fibrinogen in fibrin monomers (Ferreira, 2014). This heterologous sealant have been tested with success in animals and human beings (Gatti *et al.*, 2011; De Oliveira Gonçalves *et al.*, 2016; Perussi Biscola *et al.*, 2016) in PNL repair this sealant has shown promising results (Vicente *et al.*, 2008; Buchaim *et al.*, 2015).

Even with advances in surgical procedures, nerve reconstructions result in only about 51% of motor recovery (Sakuma *et al.*, 2016). While many studies show that there is a morphological regeneration of the nerve and muscle, this is not associated with a functional recovery, and although there is axonal regeneration with normal morphology of NMJs, the failure of the muscular electrical activation is persistant (Sakuma *et al.*, 2016). Therefore, in addition to the nerve and muscle fibers, NMJs should also be considered in these types of analyses, as well as the functional response resulting from these interactions. The fibrin sealant emerges as a potential, risk-free adjuvant to the regeneration process, when associated to the suture, allowing for reduction in the number of points and acting as a support, contributing to the axonal growth microenvironment (Biscola *et al.*, 2017).

Therefore, the objective of this study was to evaluate the use of heterologous fibrin sealant associated with a reduced number of stitches (1 point) when compared with conventional suture (3 stitches) after ischiatic nerve injury. The morphological and functional aspects of neuromuscular interaction were evaluated.

2. Materials and Methods

The study was approved by the Animal Research Ethics Committee of the Botucatu Medical School, UNESP, Brazil, under protocol no.1172/2016. Thirty - six male adult Wistar rats (UNESP / Botucatu / SP / Brazil) weighing between 300 - 400g, were divided into 4 experimental groups: 1- Control (C); 2- Denervated (D); 3- Suture (S); 4- Suture + Fibrin Sealant (SFS). Animals were kept in an environment with controlled temperature and light.

2.1 Surgical Procedure

The rats were anesthetized by I.P. (intraperitoneal) injection of Ketamine (Dopalen - 90mg / kg) and Xylazine (Rompun - 10mg / kg) and the right ischiatic nerves were exposed. Nerve injury was performed by complete transection of the nerve using a standard method, about 3 mm distal to its place of origin in the Denervated (D), Suture (S) and Suture + Fibrin Sealant (SFS) groups. In the group D, in order to avoid spontaneous regeneration, a 6 mm fragment of the sciatic nerve was removed. Upon neurotmesis, the proximal and distal stumps were inverted 180 degrees and fixed in the adjacent musculature, and sutured with simple points such as the soft tissues. In the group C, after localization of the sciatic nerve, the skin was sutured.

Seven days after neurotmesis, a new incision was made, and the nerve stumps were subjected to end-to-end neurorraphy. In the Suture group, three single points of Mononylon 7-0 were used and in the Suture + Fibrin Sealant group (SFS) one point of suture was used, in addition to 100 µL of Heterologous Fibrin Sealant (CEVAP/Brazil), which has its components and application formula listed in the patents (Registration numbers: BR1020140114327 and BR1020140114360) (Gasparotto, Vinícius Po *et al.*, 2014). Sixty days after nerve reconstruction, all animals were weighed and anesthetized by intraperitoneal injection of Ketamine (Dopalen 90mg/Kg) and Xilazine (Rompun 10 mg/Kg) to perform eleneuromyography and then euthanized with tiophental sodim (50mg/Kg). The right soleus muscle were dissected, weighed and their middle third were separeted, individually. The proximal and distal portions of the soleus muscle were frozen in liquid nitrogen and stored in a biofreezer, at -80°C. The ischiatic nerve and muscle branch of the tibial nerve for the soleus muscle were also collected.

2.2 Electroneuromyography

This analysis was performed in groups C, S and SFS; in group D, the lack of integrity of the ischiatic nerve prevented this study. The active electrode was inserted into the ischiatic nerve proximal to injury, the reference electrode in the cranial tibial muscle, and the dispersive was introduced into the trunk (distant from the test site). Amplitude and latency were recorded simultaneously (Sapphire II 4ME / UNIPEX / Botucatu / SP / Brazil).

2.3 Gait analysis using the "Catwalk" system

This evaluation was performed before surgery, and on the 15th, 30th and 60th days after sectioning and nerve reconstruction in all animals according to the experimental groups. A Catwalk XT 9.1-Noldus system was used, where the animal crossed an illuminated glass platform, monitored by a video camera associated with a footprint analysis software. The functional index of the fibular nerve (Bain *et al.*, 1989) was obtained using the following formula: PFI = 174.9 ((EPL-NPL) / NPL) + 80.3 x (ETS-NTS) / NTS) - 13.4, in which E refers to the injured side and N to the uninjured side, TS refers to the distance between the first and fifth fingers (toe spread) and PL to the distance between the third finger and the heel (print lenght). For the other parameters, the results were expressed as mean of the ratios of the injured / uninjured sides of the plantar impressions, in order to perform and analyze the gait of the animal more completely.

2.4 Morphological and morphometric analysis of the sciatic nerve and the tibial nerve muscle branch for the soleus muscle

After removal the nerves were fixed in Karnovsky and postfixed and stained with 1% osmium tetroxide. Cross sections of approximately 2 µm were obtained and photomicrographs were taken (Olympus Bx41, SC30 camera). Five random fields were used for morphometric analysis of the sciatic nerve (5% of the sample); for the tibial nerve the whole sample was used. The number, diameter and area of the axons and the nerve fibers were obtained, and from these, the thickness of the myelin sheath and the G-ratio were calculated. For the calculation of the number of axons and nerve fibers of the sciatic nerve, we used a ratio witch considered the calculated sample in relation to the total nerve (Sobral *et al.*, 2008).

2.5 Analysis of muscle fibers and percentage of collagen (n = 5)

In the proximal portions of the frozen soleus muscle, microtomy (8 µm), was performed, and 4 slides were prepared for each animal in each experimental group: first-HE, second-Picrossirius Red and third and fourth immunohistochemistry for Fast and Slow fibers, respectively. Slides were photographed at 200X magnification (Olympus Bx41, SC30 camera). HE staining was used for overall morphological analysis and morphometry of the muscle fibers area (200 muscle fibers from 3-4 random fields). This analysis was performed using “Image J” software (Schneider *et al.*, 2012). Slides stained with Picrossirius Red was used to quantify the percentage of collagen (Leica QWin software) where automatic detection of red were used to determine the percentage of collagen. The third and fourth sides were subjected to immunohistochemistry using specific primary antibodies (Anti-myosin fast/Novocastra/1:130 and Anti-myosin slow/Novocastra/1:180). Histofine® (Multi-Nichirei) was used as the secondary antibody. The specific staining was revealed by the chromogenic substrate DAB (1:50). The frequency of muscle fiber types was calculated using the “Image J” software (Schneider *et al.*, 2012).

2.6 Protein quantification (Western Blotting) of PCNA (cell proliferation) and PAX7 (satellite cells), n = 5.

The distal portions of the soleus muscle were homogenized in RIPA and protease inhibitors (30mg of tissue/100µl of extraction buffer). Tissue extracts were obtained by centrifugation for 10 minutes at 1,4000 rpm at 4ºC. Protein content was determined by the Bradford method (Bio-Rad protein assay) and 75 micrograms of protein was used for analysis in polyacrylamide gel. After electrophoresis, the material was transferred to nitrocellulose membranes followed by blocking with 3% skim milk in TBS-T for one hour and then incubated with the primary antibodies (PaX7 / ab199010 1: 200-PCNA / ab29 / 1 : 150). Following the wash step, the membranes were incubated for one hour in secondary antibody HRP and revealed using a quimioluminescent substrate for Western blotting (AMERSHAM ECLTM PRIME, GE Healthcare). Semiquantitative analysis of band densitometry was performed by Image J. Software (Schneider *et al.*, 2012). Data were normalized using GAPDH (Cell Signaling).

2.7 Morphological and morphometric analysis of NMJs by light microscopy (nonspecific esterase), (n = 5)

The middle third of the right soleus muscles was fixed in Karnovsky's solution, sectioned longitudinally with razor blade and subjected to the Non-specific Esterase reaction (Lehrer e Ornstein, 1959), in order to characterize NMJs. Slides were photographed (200 x)-(Olympus Bx41(camera SC30) and measurements were taken from the area of 50 NMJs, which were analyzed using "Image J" (Schneider *et al.*, 2012).

2.8 Ultrastructural analysis of muscle fibers and neuromuscular junctions (NMJs), (n = 3)

The muscular thirds were reduced into rectangular fragments in order to obtain longitudinal sections of the associated fibers and NMJs. This material was processed and photodocumented according to the routine of the Electronic Microscopy Center of the Institute of Biosciences (CME / IBB / UNESP) in an Electronic Transmission Microscope (TECNAI Spirit Fei Company).

2.9 Statistical analysis

The results were expressed as a mean and standard deviation, and statistically significant differences were considered when $p < 0.05$. For the analysis of Amplitude and Latency, area and diameter of axons and nerve fibers, myelin sheath thickness, G ratio, soleus muscle weight, collagen percentage, protein quantification of Pax7 and PCNA and muscle fiber area and JNMs, analysis of variance for the model with one fator were applied complemented by Tukey's multiple comparison test (Zar, 2009). For analysis of animal weight and time of contact, it was used analysis of variance for the model of repeated measurements in independent groups complemented by the multiple comparisons test of Bonferroni (Johnson e Wichern, 2014). For the number of axons and nerve fibers, a non-parametric analysis of variance (Kruskal-Wallis) was used for the model with a factor complemented with by Dunn's multiple comparison test (Zar, 2009). For the area of the footprint, the ratio of maximum contact area and the Fibular Functional Index, a nonparametric analysis of variance was used for the replicate measures model in independent groups complemented by Dunn's multiple comparison test (Johnson e Wichern, 2014).

3. Results

3.1 Electroneuromyography*

Electroneuromyography analysis was performed in the animals of groups C, S and SFS, through which amplitude and latency values were obtained. Regarding Amplitude, mean values were higher in group C (23.04 ± 6.52) when compared with S (7.10 ± 4.56) and SFS (8.40 ± 5.46) (Figure 1-A). The mean values of the Latency values were lower in group C (1.39 ± 0.40), compared with the lesion groups: S (2.59 ± 0.74) and SFS (2.66 ± 1.51) (Figure 1-B). The lesion (S and SFS) groups did not show statistical differences when compared with the electroneuromyography parameters analyzed.

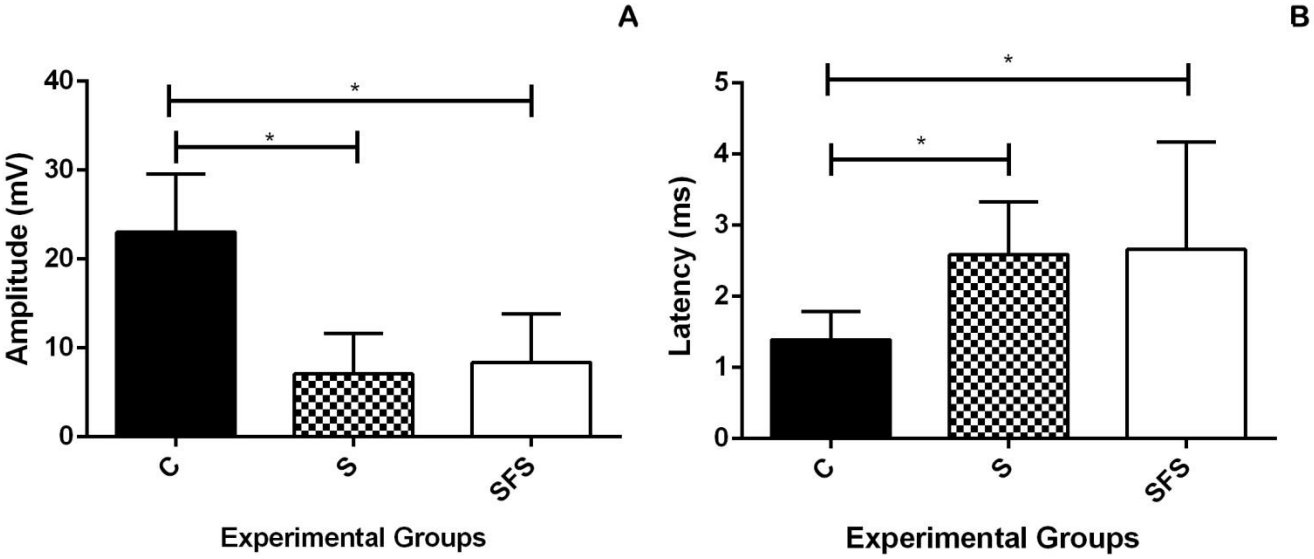

Fig. 1: Graph showing Mean ± Standard Deviation (SD) of the Amplitude and Latency values in all experimental groups. A: amplitude values (mV); B: latency (ms); (Technique of analysis of variance for the model with one factor complemented by Tukey test of multiple comparisons (Zar, 2009), *p< 0.05).

***This analysis was not performed in the group D animals, due to the absence of integrity of the sciatic nerve.**

3.2 Evaluation of animal gait using the *"*Catwalk*"*

Gait parameters, assessed before surgery, did not show differences in all animals from all experimental groups. On the 15th day, post surgery, there was a difference between the groups when we compared the ratios of the footprint areas, with the higher ratio found in group C animals, followed by group D. The lower values were detected in the groups S and SFS. On the 30th postoperative day, the footprint ratios followed the same pattern described on the 15th day for the experimental groups (Figure 2-B).

The other parameters also showed differences on the 30th day. The ratio of contact time was lower in all experimental groups when compared with C (Figure 2-A). The highest values in relation to the ratio of the maximum contact area of the legs with the platform were observed in group C, followed by group D, with the lowest values shown by groups S and SFS (Figure 2-C). Regarding the Functional Index of the Fibular, the highest values were those of the groups C and D, whereas the groups S and SFS had the lowest values (Figure 2-D).

On the 60th postoperative day, the groups D, S and SFS had lower values when compared with group C in relation to the areas of maximum contact and footprint and in the functional index of the Fibular nerve (Figure 2- B, C and D). The ratio of contact time was higher in group C, followed by group S. Groups D and SFS had the lowest values related to this parameter (Figure 2-A).

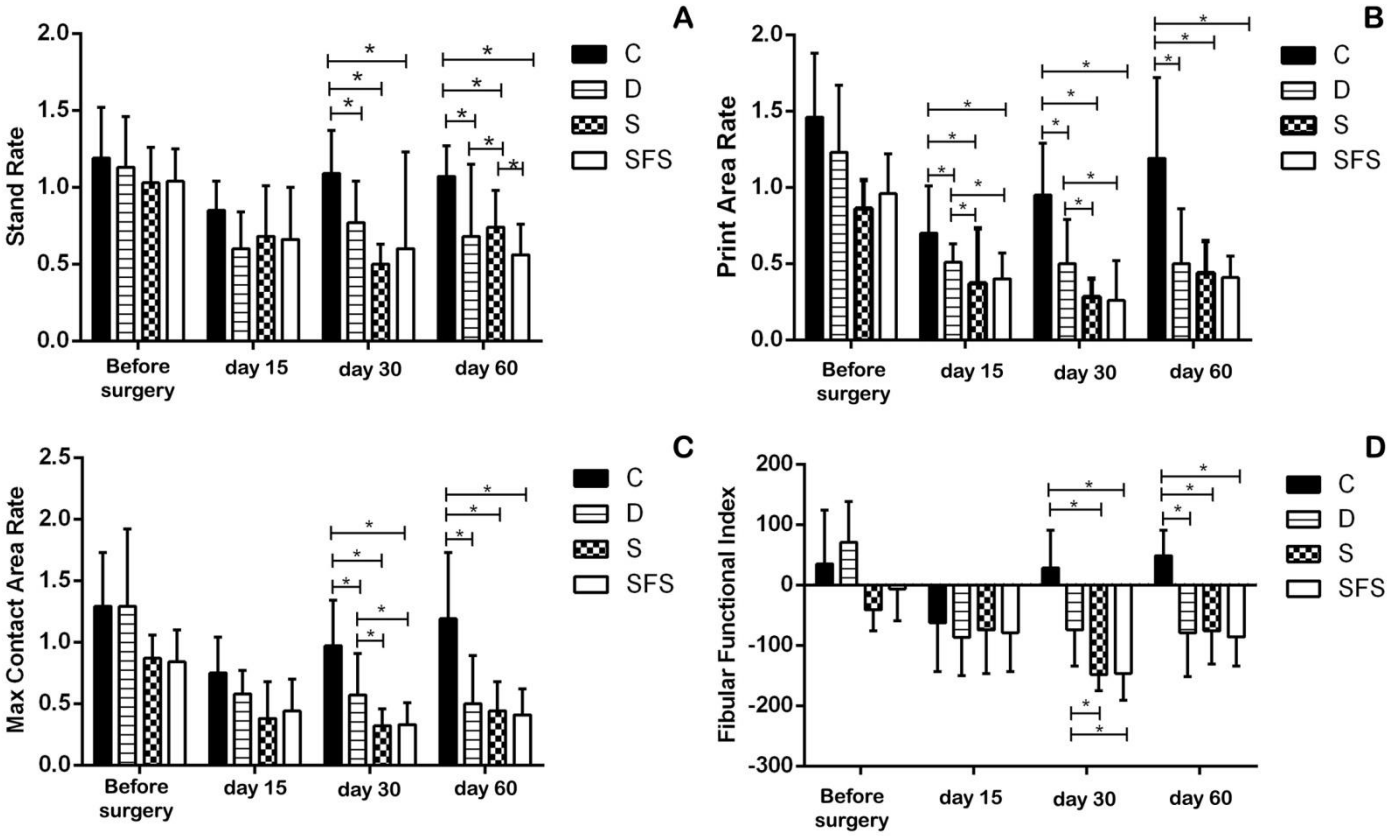

Fig. 2: Graphs of the means and standard deviation of the functional analyses (Catwalk) for the experimental groups at the different times. A: Ratio of contact time; B: Ratio of the footprint area (cm); C: Ratio of maximum contact area; D: Functional Fibular Index. The values in A, B, C are expressed as the ratio of the injured/uninjured sides of the plantar impressions. In A: Technique for analysis of variance for the model of repeated measurements in independent groups complemented by the Bonferroni multiple comparison test (Johnson & Wichern, 2007), * p <0.05. In B, C and D: nonparametric analysis of variance for the repeated measures model in independent groups complemented by Dunn's multiple comparison test (Johnson & Wichern, 2007), *p< 0.05.

3.3 Weight of the animals and of the soleus muscle.

The final weight of the animals from all experimental groups was statistically significantly higher when compared to their initial weight. When the groups were compared, there was no difference between them at the beginning and at the end of the experiment. Regarding the weight of the soleus muscle, group C animals had the higher values, followed by animals from the groups S and SFS. In these groups, the weight of the soleus muscle was statistically similar between them, and different from the other groups, showing lower values compared with group C and higher values compared to group D, which in turn had the lowest value (Figure 3).

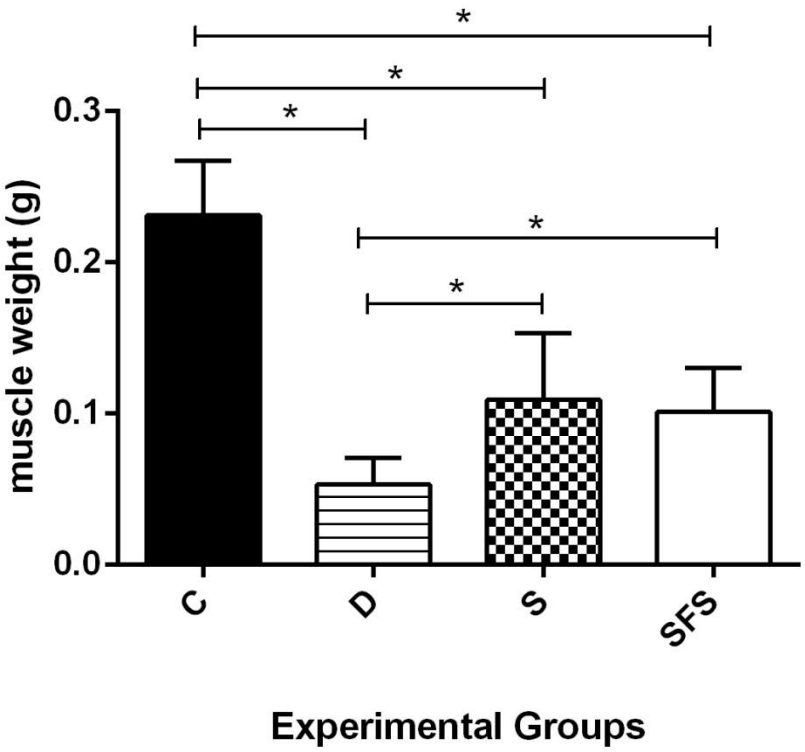

Fig. 3: Graph of the means and weight deviation (g) of soleus muscle in all experimental groups.
(Technique of analysis of variance for the model with one factor complemented by test of multiple comparisons of Tukey (Zar, 2009), *p< 0.05).

3.4 Morphological and morphometric analysis of the ischiatic nerve and the tibial nerve muscle branch for the soleus muscle*

Histological images of both nerves in group C showed an axon and integral myelin sheath, with morphology within the normality pattern (Figure 4-A e 5-A). The tibial nerve general morphology was indicative of degeneration in group D (Figure 5-B). In the ischiatic nerve it was not possible to identify axons and nerve fibers. In S and SFS groups, in relation to both nerves, the morphology showed axons and nerve fibers remielinizated when compared with group D, although the axons seemed to be smaller and irregular in relation to C (Figure 4-B and C and 5-C and D).

In the morphometric analysis of the ischiatic nerve, the values referring to the axon area, fiber area and axon diameter showed the same statistical pattern, with the highest values presented by group C, followed by the values of the SFS group, and with the group S having the lowest values among all groups (Figure 4-D,E and G). Regarding the diameter of the nerve fibers, the groups C and SFS showed similar results, followed by the lower values shown by group S (Figure 4-H). Regarding the number of axons and fibers, the highest values were those of group C, followed by the values of groups S and SFS, with no difference between them (Figure 4-F). The results of myelin sheath thickness and G ratio were statistically similar in the 3 experimental groups (C,S e SFS) (Figure 4 I and J).

The morphometric analysis of the tibial nerve revealed a statistical pattern among the groups where the values for the number of nerve fibers and axons, area of nerve fibers and axons, minimum diameter of nerve fibers and axons and thickness of myelin sheath showed higher values in the animals of group C when compared to the groups S and SFS (Figure 5 E - J). The G ratio values were lower in group C when compared with S and SFS groups (Figure 5 K). On the other hand, the animals of the lesion group (S and SFS) were not statistically significantly different when the parameters described above were analyzed.

***This analysis was not performed in group D animals, due to the absence of regenerated nerve fibers.**

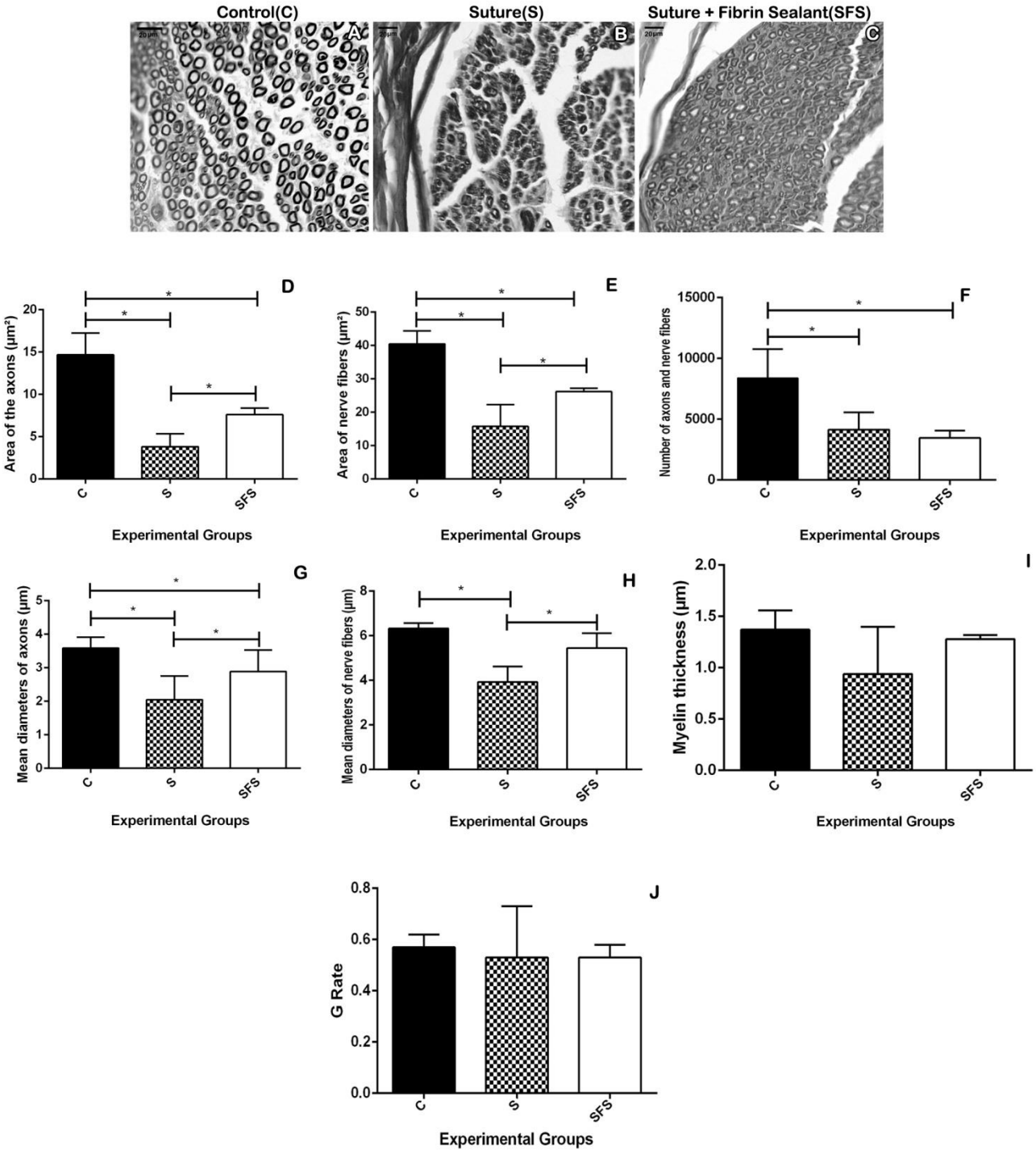

Fig. 4: A-D: Photomicrographs of transverse sections of ischiatic nerve, stained in osmium tetroxide. A: Control group (C); B: Denervated group (D); C: Suture group (S); D: Suture + Fibrin Sealant (SFS). D-J: Graphs showing the Mean and Standard Deviation values corresponding to the morphometric analysis of the sciatic nerve in the groups C,S and SFS. D: Area of axons (μm^2); E: Area of nerve fibers (μm^2); F: number of axons and nerve fibers. G: diameter of the axon (µm); H: diameter of nerve fibers (µm); I: Thickness of myelin sheath (µm); J: ratio G. D,E,G-J : Technique of analysis of variance for the model with one factor complemented by test of multiple comparisons of Tukey (Zar, 2009), *p< 0.05. F: Technique for analysis of non-parametric variance (Kruskal-Wallis test) for the model with factor complemented by Dunn's multiple comparison test (Zar, 2009),* p< 0.05).

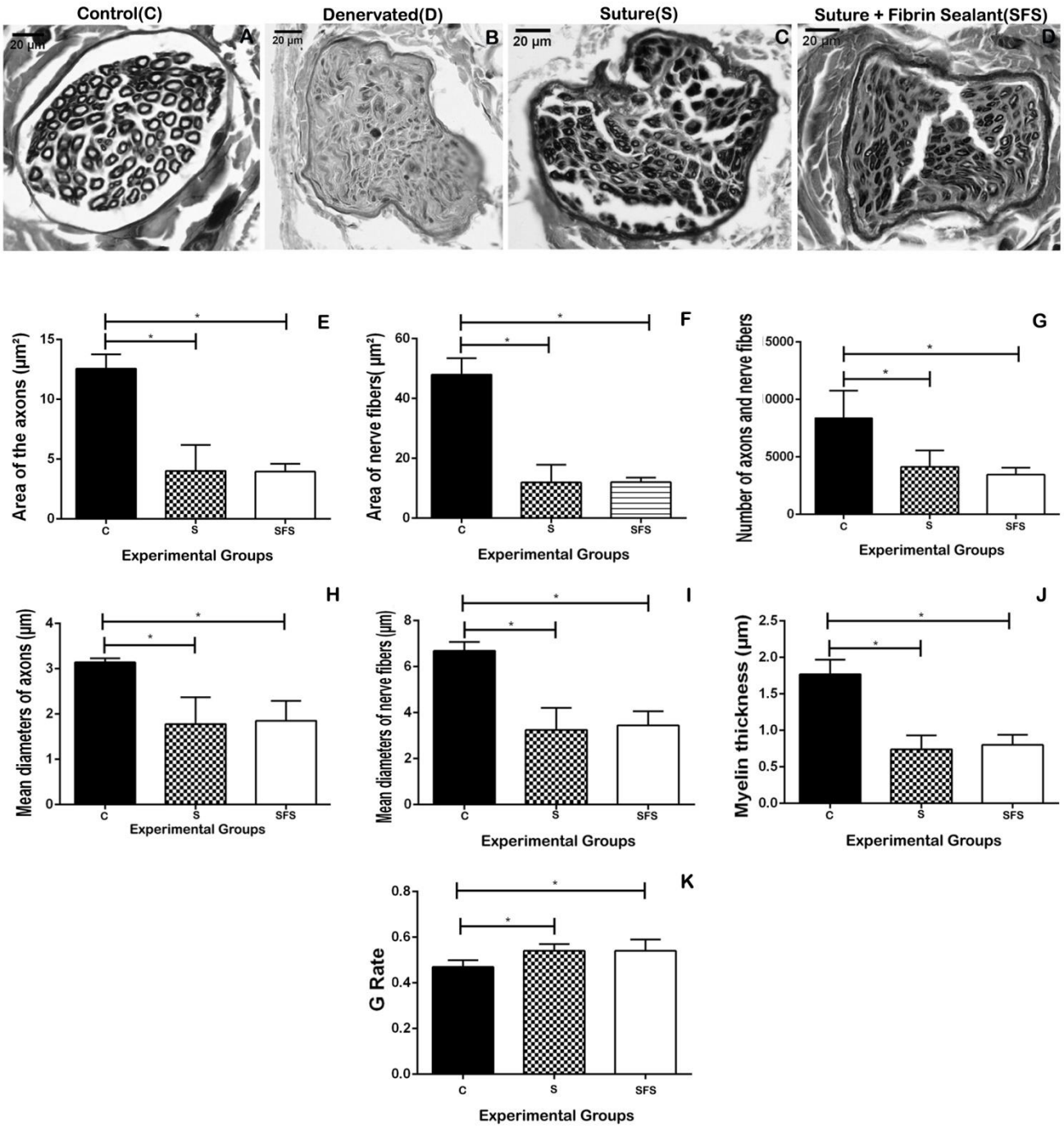

Fig. 5: A-D: Photomicrographs of transverse sections of the tibial nerve muscle branch, stained in osmium tetroxide. A: Control group (C); B: Denervated group (D); C: Suture group (S); D: Suture + Fibrin Sealant group (SFS). E-K: Graphs of the means and standard deviation of the morphometric analysis of the muscle branch of the tibial nerve for the soleus muscle of the C, S and SFS groups. E: Area of axons (µm2); F: Area of nerve fibers (µm2); G: number of axons and nerve fibers. H: axon diameter (µm); I: nerve fiber diameter (µm); J: Thickness of myelin sheath (µm); K: ratio G. E,F,H-K : Technique of analysis of variance for the model with one factor complemented by test of multiple comparisons of Tukey (Zar, 2009), *p< 0.05. G: Technique for analysis of non-parametric variance (Kruskal-Wallis test) for the model with factor complemented by Dunn's multiple comparison test (Zar, 2009),* p< 0.05).

3.5 Analysis of muscle fibers and percentage of collagen

In group C, the morphological analysis performed after HE staining showed characteristics compatible with normality: muscle fibers in polygonal format and with peripheral nuclei (Figure 6A). Ultrastructurally, the myofibrils were well organized forming intact sarcomeres with morphological characteristics closely related to the different muscle types. A linear Z-line, intermiofibrillary mitochondria of variable sizes and T-tubules organized in triads were highlighted, as well as peripheral nuclei (Figure 7A).

HE staining analysis showed, in group D, agglomerates of small fibers, some of them with a rounded shape and others with a central nucleus (Figure 6B). Ultrastructurally, in most myofibrils there was no organization in sarcomeres, with some regions containing only bundles of myofibrils, and a fragmented and scattered Z-line. Focal areas of lesion were present showing myelin figures and concentration of mitochondria; and central nuclei were abundant (Figure 7B).

An intermediate morphology was observed in the S and SFS groups, with fibers with rounded shape and others with central nuclei visualized by HE staining (Figures 6C and 6D). The ultrastructure revealed the recovery of muscle tissue where the sarcomeres were organized; focal areas of lesion were still present. The presence of papillary projections on the surface of the muscle fiber membrane was also observed in groups D, S and SFS (Figures 7C and 7D).

Regarding the fiber area, group C animals showed the highest values. The animals in groups D and SFS presented the lowest values, and those in group S had intermediate values (Figure 6E).

Group D presented the highest percentage of collagen, followed by groups S and SFS, while group C had the lowest percentage values (Figure 6F).

By the immunohistochemical staining, it was observed that the types of muscular fibers of group C were organized in a mosaic. In groups D, S and SFS there were areas with grouping of fiber types ("Type grouping") (Figure 8-F). In relation to the frequency of Slow fiber types, group C (183/155; 198) had the highest amount of this type of fibers, being statistically superior to the others; the animals of groups D (143/125; 181) and SFS (153/85; 172) showed intermediate values, which were similar to each other and different from the other groups. The lowest values were those presented by group S (134/123; 163), which were still statistically inferior

to the others (Figure 8-D). The frequency of the Fast fibers was higher in the SFS group (76/40; 127), followed by the D (58/57; 77) and S (75/49; 93) groups; while group C had the lowest values (28/24; 55) (Figure 8-E).

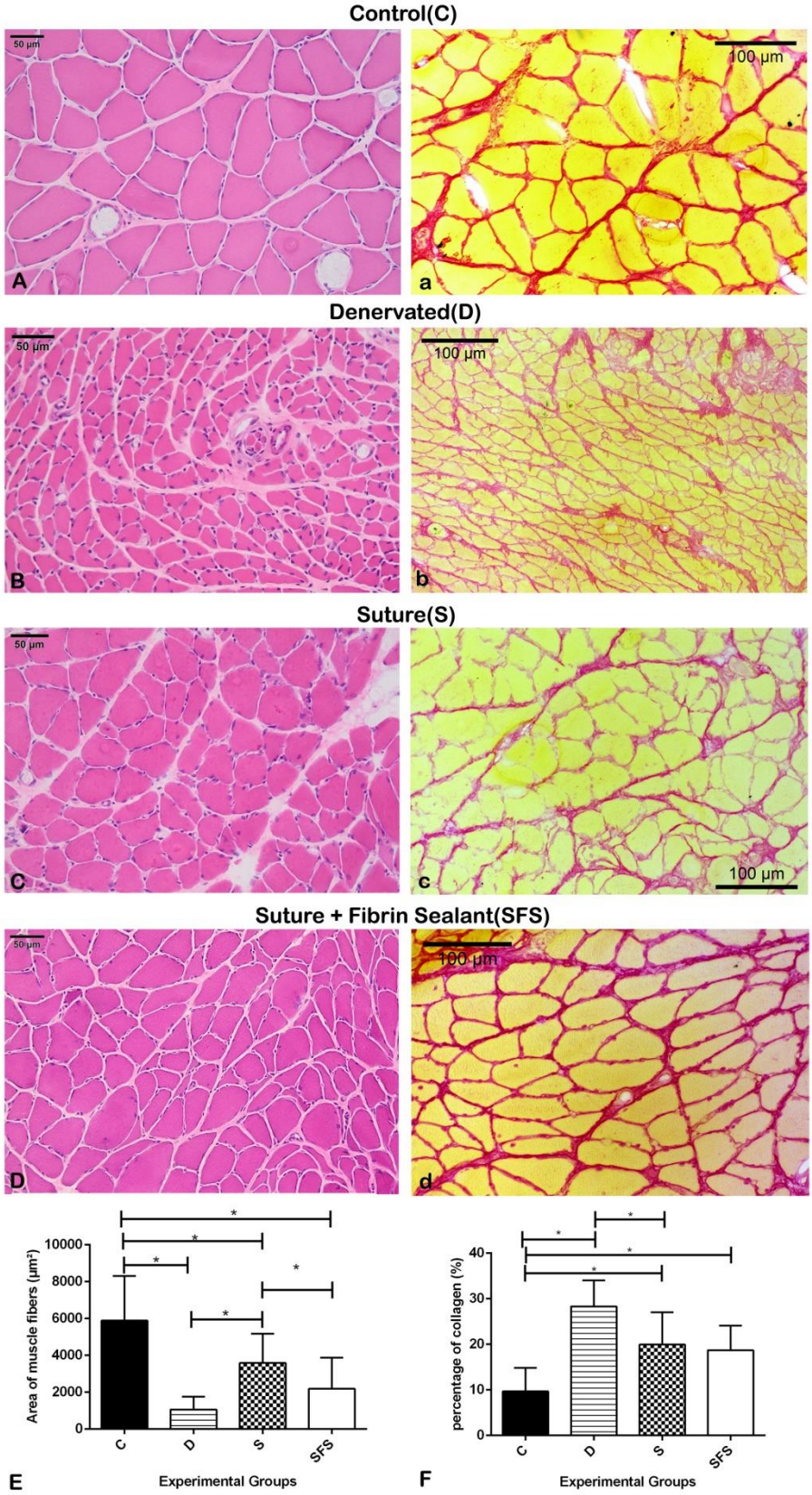

Fig. 6: (A-D) Photomicrographs of cross sections of the soleus muscle stained with HE and Picrossirius Red (a-d) from all experimental groups, under conventional light microscopy. (E) Graph of the Mean and Standard Deviation values of the area of muscle fibers for all experimental groups. ($p < 0.05$, technique for analysis of variance for the one-factor model complemented by the Tukey's multiple comparison test). (F) Graph of the percentage of collagen for all experimental groups. (Technique of analysis of variance for the model with one factor complemented by the Tukey's multiple comparison test (Zar, 2009, *$p < 0.05$).

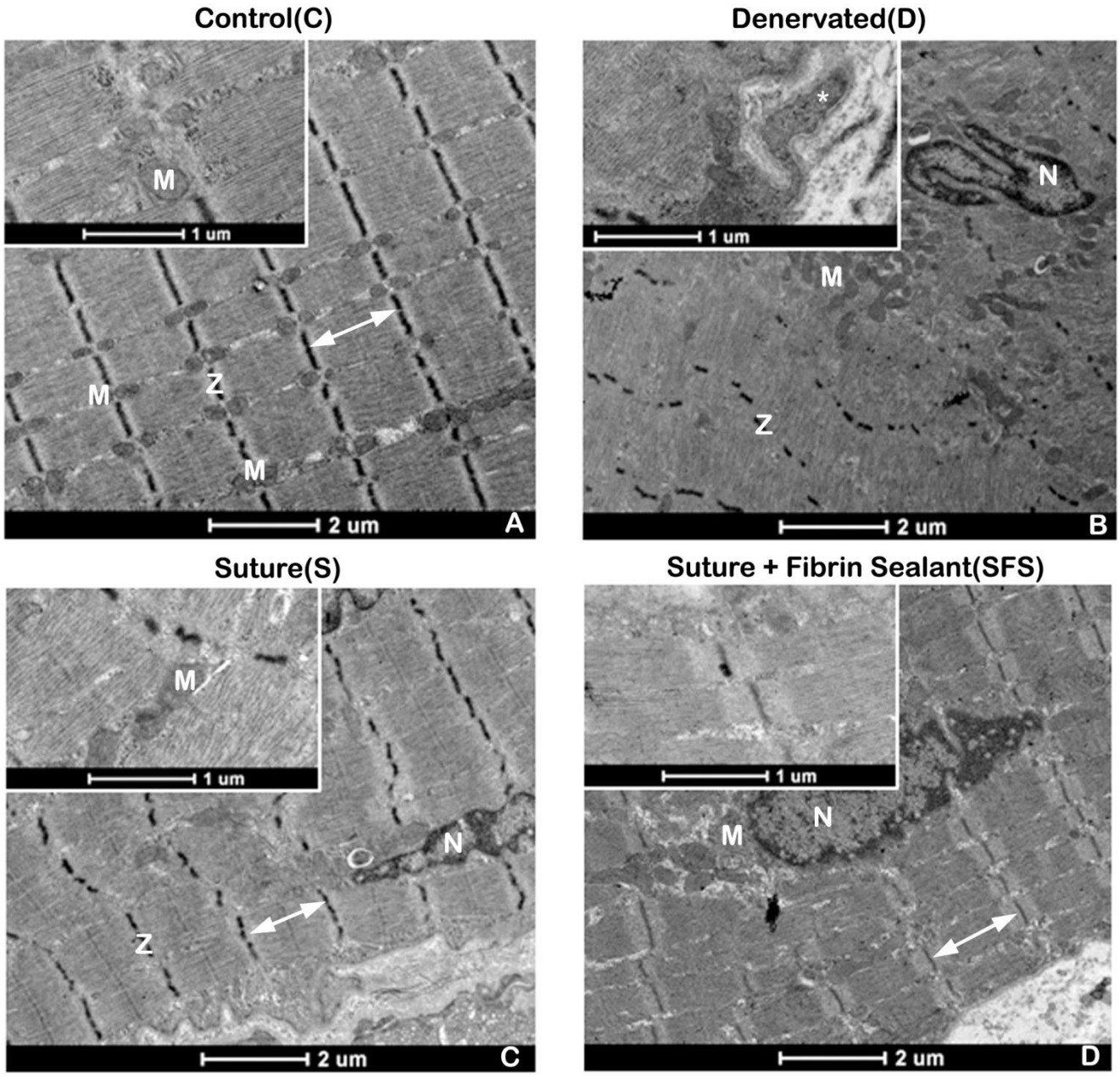

Fig. 7: Electron micrographs of muscle fibers; (M) mitochondria, (Z) Z-line, (↔) sarcomeres, (N) Nuclei.

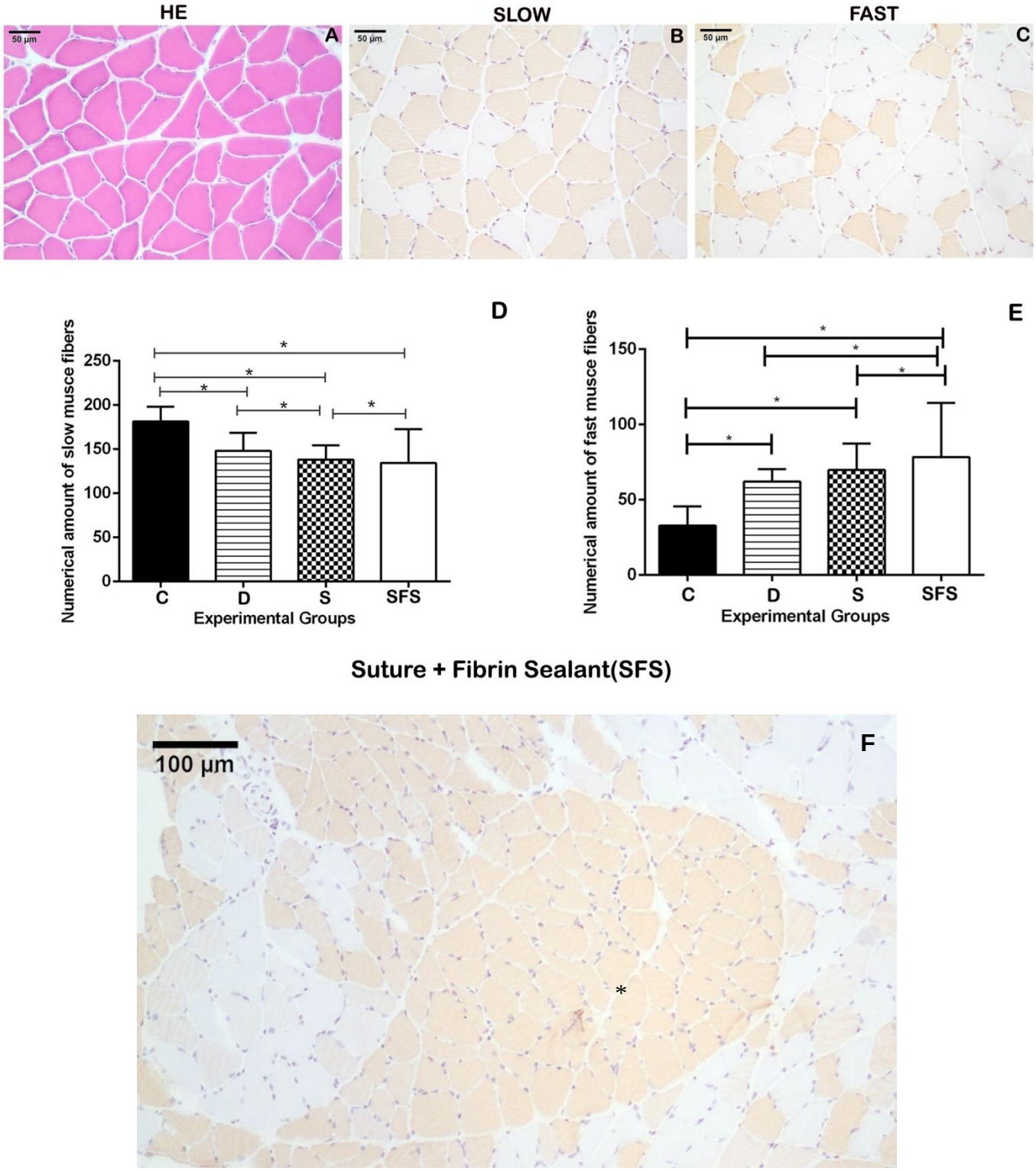

Figura 8: A-C: Photomicrographs of transversal sections of the soleus muscle of the control group. A: HE; B: Immunohistochemistry for Slow Fiber; C: Immunohistochemistry for Fast Fiber. D and E: Graphs of the Mean and Standard Deviation values of thE frequencies of Fast and Slow fiber types, respectively (technique of the non-parametric analysis of variance for the model of repeated measures in independent groups complemented by Dunn's multiple comparison test (Johnson & Wichern, 2007), *p< 0.05). F: Cross-sectional photomicrography of the soleus muscle of the SFS group. Immunohistochemistry for Fast Fiber. Asterisk: fibers in "Type grouping".

3.6 Protein quantification (Western Blotting) of PCNA (cell proliferation) and PAX7 (satellite cells)

Regarding quantification of PCNA and PAX7 proteins, there was no statistically significant difference between the experimental groups.

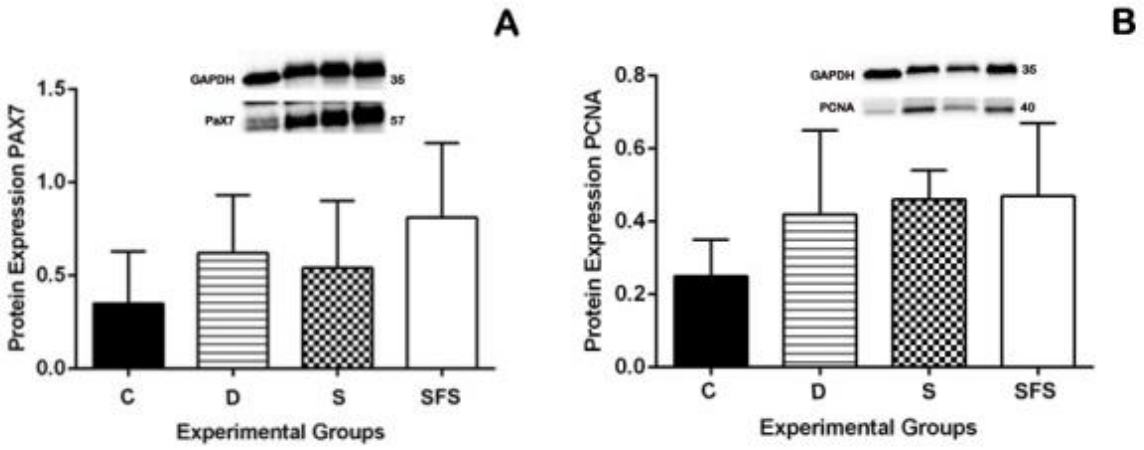

Fig. 9: Graphs of the means and standard deviation of the protein quantification of PaX7 (satellite cell marker) and PCNA (cell proliferation). Detail: protein expression of PaX7 and PCNA, respectively. (Technique of analysis of variance for the model with one factor complemented with the Tukey's multiple comparison test (Zar, 2009), *p< 0.05).

3.7 Morphological and morphometric analysis of NMJs

Using the non-specific esterase, was observed that the NMJs were aligned to the largest axis of the muscle fibers, in all animals of the experimental groups.

In group C, its distribution was restricted to the muscular middle third, with a highly branched, broad synaptic gutter with transverse striations corresponding to the junctional folds (Figure 10-A). Ultrastructurally, several synaptic knobs were observed, arranged in synaptic gutter with varied shapes and depth. In the synaptic bottons, synaptic vesicles, mitochondria and multivesicular bodies were present. Characteristically, the presynaptic membrane had more electrondense regions that correspond to the active zones, opposite the apex of the junction folds of the postsynaptic membrane. The post-synaptic membrane was intact and contained numerous long junctions, with a more electron-dense apex corresponding to the site of concentration of acetylcholine receptors (Figure 11-A).

In group D, the appearance was compact and broad, with NMJs sparsely distributed in relation to the middle third (Figure 10-B). Degeneration of the pre-synaptic region was detected through the ultrastructure, leaving only junction folds, and it was not possible to distinguish the active zone (Figure 11-B).

In the S and SFS groups the morphology was intermediate to the previous ones, with distribution of NMJs in addition to the middle third (Figure 10-C and D). Some synaptic gutter observed ultrastructurally were unoccupied, although some synaptic knobs presented variable morphology. Myelin figures, large numbers of synaptic vesicles and cellular debris were present. At the apex of the junction folds small regions of variable electron density were detected (nACRs concentration) (Figure 11-C and D).

The NMJ area presented lower values in group D animals when compared with group C ($p = 0.03$). The groups S and SFS did not show differences between themselves and in relation to the other groups (Figure 10-E)

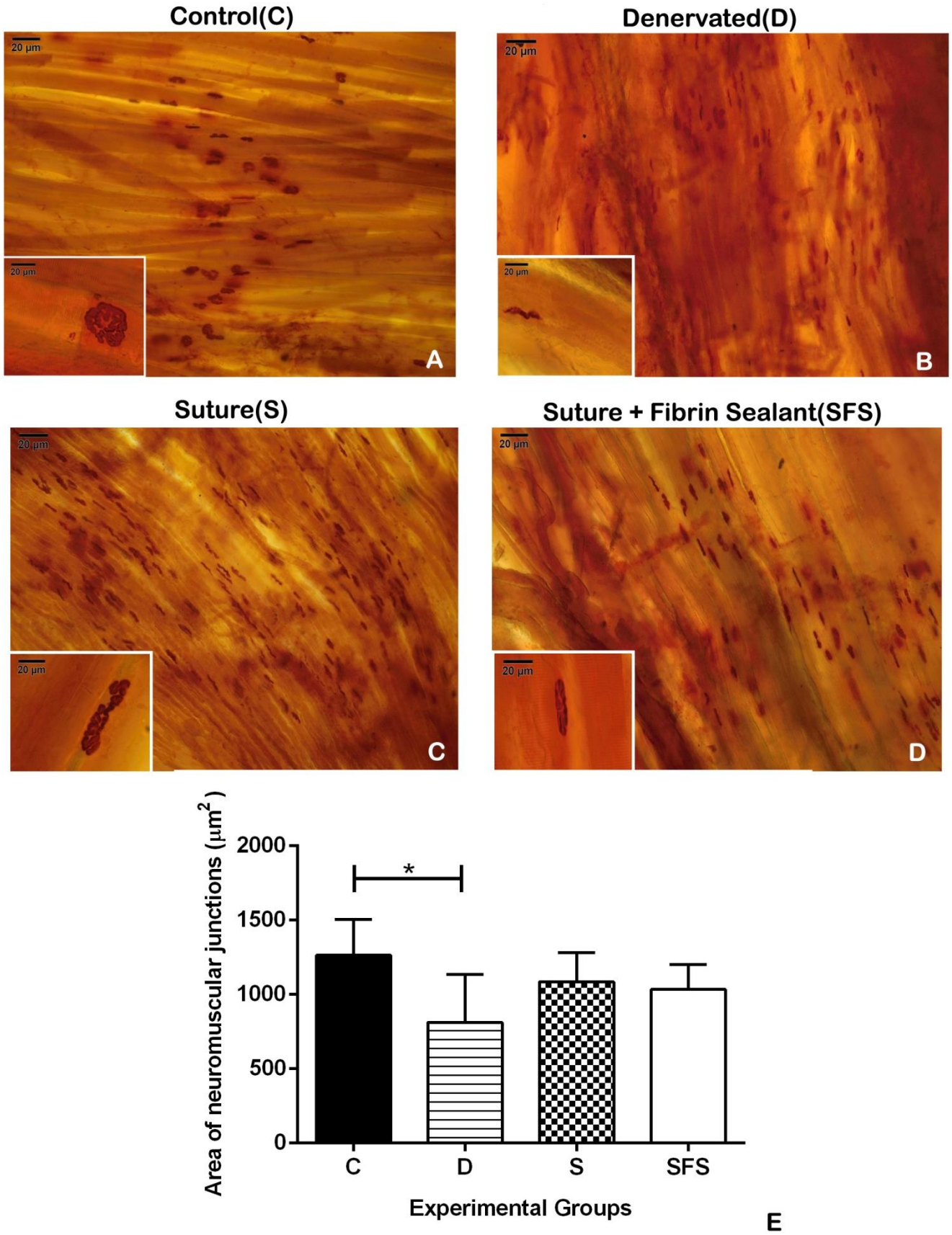

Figure 10: A-D: Photomicrographs of the right soleus muscle (total assembly) of all experimental groups. NMJs labeled with non-specific esterase. Detail: NMJs. E: Graph of the means and standard deviation of the JNMs area (µm2) for all experimental groups. (Technique of analysis of variance for the model with a factor complemented by the Tukey's test for multiple comparisons (Zar, 2009), *p< 0.05).

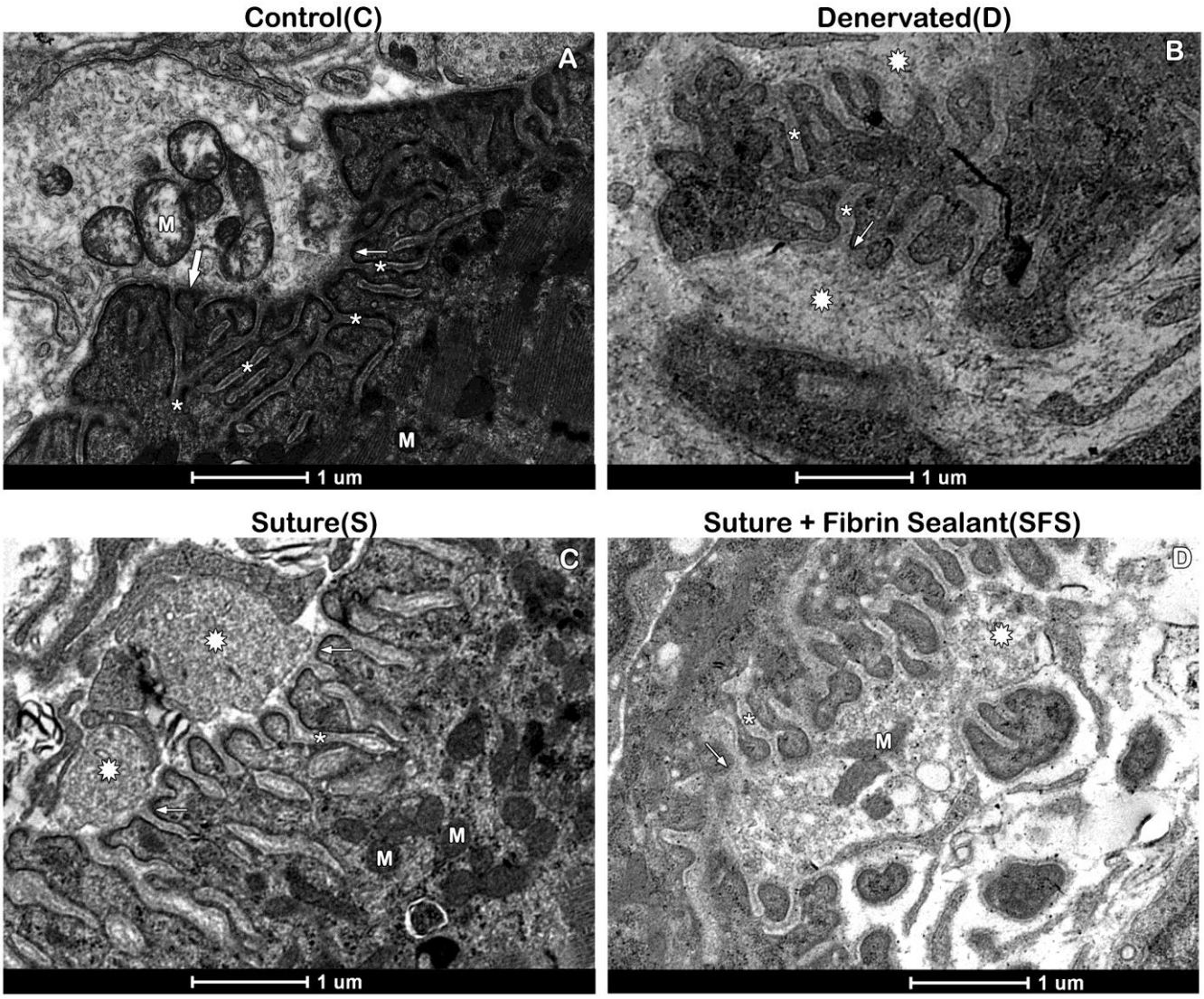

Fig. 11: Electron micrographs of NMJs. (M) mitochondria,(✪)synaptic button,(➡)active zone, (*) junction folds and (→) concentration of nAChRs.

4. Discussion

In this study, the model of nerve injury chosen was the complete transection of the ischiatic nerve (neurotmese), followed by burial of the nervous stumps next to the adjacent musculature. This type of model was chosen considering that neurotmesis is the most severe form of peripheral nerve injury, with no complete functional recovery (Grinsell e Keating, 2014). The burial of stumps was performed to avoid spontaneous regeneration, considering that the peripheral nervous system has a remarkable ability to regenerate after nerve damage, even though the distance between the stumps resulting from injury restrain axonal growth, limit the regeneration process (Gaudet *et al.*, 2011). In the search for new methods, in order to achieve better morphological and functional recovery, the association of the new fibrin sealant (CEVAP) at only one point of suture, which reduces the points used in the conventional technique, has been chosen in this study as a methodology for nerve reconstruction. This sealant, developed by CEVAP, Unesp, Botucatu, SP, Brazil, has the singularity of being free of human blood, which makes the CEVAP fibrin sealant a distinct product from the existing, commercially available ones, having the important advantage of reduced adverse reactions (Biscola *et al.*, 2017).

The period of 7 days for post-injury reconstruction was chosen in order to observe the action of the sealant used, given that after this period nervous degeneration is well established (Tricaud e Park, 2017). In addition, although delayed nerve reconstruction is expected to impair recovery (Coulet *et al.*, 2010), this type of injury is commonly accompanied by other major trauma requiring urgent treatment; so the choice of this period can simulate this real life situation.

In this study, the option to fix the stumps to the adjacent musculature after neurotmese may have provided the Denervated group with a condition for collateral reinnervation, whose functional results in relation to the ratios of the footprint area (15 and 30 days post-surgery) and contact (30 days post-surgery) obtained with the Catwalk, were higher than those of the S and SFS groups. This neurotization process is defined by the viability of muscle contraction through nerve stimuli by nerves or by other, non directly related muscles (Giordani *et al.*, 2009). In this group it was possible to observe morphological characteristics indicative of atrophy, already well described in the literature, which result from denervation: reduction of muscle weight (Michael *et al.*, 2012; Higashino *et al.*, 2013; Frost *et al.*, 2016) and of the area of fibers (Wiberg *et al.*, 2015; Tuffaha *et al.*, 2016; Ohira *et al.*, 2017), increase in the

percentage of collagen (Nikolaou *et al.*, 2014; Pinheiro-Dardis e Russo, 2017), central nuclei (Su *et al.*, 2016); ultraestructurally desaggregation of sarcomeres, and a discontinuous and fragmented Z line were observed (Sakakima *et al.*, 2000). Regarding NMJs, analysis of this area was statistically smaller when compared with group C, a finding compatible with the reduction of muscle fiber diameter (Confortim *et al.*, 2015); ultraestructurally, empty sinaptic gutter were observed (Sakakima *et al.*, 2000).

Electroneuromyography data on amplitude and latency showed that group C had the best values, with recovery in groups S and SFS without, however reaching the values of the control group, where latency values that refer to the speed of nerve conduction were low and the Amplitude values were high, which relate to the number of muscle fibers that are able to respond to the electrical stimulus and, consequently, to the number of excitable axons.

Martins et al (2005), in an experimental study comparing the exclusive use of suture and associating a suture point with fibrin glue (commercial) for nerve reconstruction, found a similar pattern for amplitude and latency in the reconstructed groups similar to the data obtained in our study. However, the latency values indicated a higher speed of conduction, compared with those obtained in our study, probably because the period studied by these authors was longer, 24 weeks (around 170 days). The period chosen in our 60-day study was sufficient for the axons to cross the lesion site and reinerve the target organs, but for full nerve fiber maturation, a longer period might be necessary (Martins *et al.*, 2005). However, the amplitude values found in the S and SFS groups differed from those of Martins et al (2005), being higher than those of these authors, which suggested that the same nerve impulse may have stimulated a greater number of muscle fibers.

The morphological analysis of the ischiatic nerve and the muscle branch of the tibial nerve to the soleus muscle showed this same pattern of regeneration and similarity between the S and SFS groups, whose morphology was closely related to group C. Values for the diameter, area, number of axons and nerve fibers, and thickness of the myelin sheath of the tibial nerve were also similar in groups S and SFS. As for ischiatic nerve analysis, only the number of axons and nerve fibers was similar between these 2 groups, while the area and diameter values were higher in the SFS group. Both the biological sealant and the commercial sealer used, mimic the end of the coagulation cascade, providing an environment of protection and

stability in the site of reconstruction, leading to the ability to potentiate nerve regeneration (Isaacs *et al.*, 2008). The indices of myelin degeneration/regeneration were also evidenced by the G ratio found in both nerves, which were within the range of normality (between 0.4 and 0.7) for the 3 groups analyzed (C,S and SFS) (Mendonça *et al.*, 2003). These values, as well as the latency values obtained, indicate that there was remyelination of the nerve fibers. However, motor recovery results obtained by the Catwalk test showed functional deficits in all injured groups (D, S and SFS), with IFF values near -100 (Bain *et al.*, 1989). Lower values when compared to control animals in relation to the analyses of the paw area and the maximum contact area, both at the end of the experimental period (60 days), also indicate failure in the motor recovery. These last two parameters are directly related to the pressure exerted by the paw on the platform, and the values of these ratios close to zero indicate difficulty during support of the paw (Gensel *et al.*, 2006). Therefore, although the previous data are indicative of axonal regeneration, the failure shown in motor recovery may be associated with the experimental period analyzed, which may not have been sufficient to promote complete nerve recovery. Cartarozzi et al (2015) obtained similar results after 60 days of nerve reconstruction using stem cells + fibrin sealant as a repair technique. Studies which included longer periods of observation, such as 90 days (Willand *et al.*, 2015) and 180 days (Maciel *et al.*, 2013) after reconstruction with suture and electrostimulation, have reported funcional improvement.

An increase of Fast fibers was detected in groups D, S and SFS, with the SFS group showing the highest frequency of this type of fiber. According to the literature, the increase of Fast fibers is a pattern present in oxidative muscles, as the case of the muscle studied herein - the soleus muscle, being an indication of muscle plasticity in the case of peripheral nerve injury (Germinario *et al.*, 2002; Patterson *et al.*, 2006).

In these experimental groups, it is underscored the presence of areas containing "Type grouping", which is characterized by the presence of agglomerates of fibers of the same type. In general the normal muscle fiber is surrounded by approximately 6 muscle fibers that do not belong to its motor unit, however, in partially denervated muscles, the muscle fibers of the motor unit become progressively grouped with muscle fibers of the same type. This occurs because the muscle fibers of different motor units decrease as the muscle fibers of the same unit

increase due to a reduced number of axons that regenerate and reinnervate the muscles after lesions due to nerve transection (Gordon, 2016). The presence of this same pattern in the denervated animals (D), reinforces the possibility of neurotization. This change in the muscular innervation pattern after PNLs also explains the distribution beyond the middle third of the NMJs in the soleus muscle, where the emission of nodal roots of the last Ranvier node and of terminal and ultraterminal roots that emanated from intact muscle units close to the lesion (Gordon *et al.*, 2004), lead to competition during reinnervation, causing a polyneural innervation for a certain period of time (Rich e Lichtman, 1989).

Ultrastructurally, the presence of papillary projections on the membrane surface of the muscular fibers of the D, S and SFS groups suggestive of muscular atrophy (Engel e Orawa, 2004), together with the presence of focal lesion areas still present in the S and SFS groups, are also indicative that the muscle regeneration process is not yet complete 60 days after the injury. This may also explain the fiber area results, where the values present in the SFS group were close to the values in group D. The heterogeneity found in relation to the fiber size in the SFS group, by inscreasing the standard deviation, may have contributed to this similarity. In addition, in this group, fibers with large diameters, of rounded shape, have been observed, which have been found in muscular dystrophies, after trauma and as a result of atrophy after denervation (Bonnemann e Bushby, 2004).

The remaining morphological results showed a recovery in the animals of the S and SFS groups compared to the animals of the Denervated group, exemplified by an increase in muscle weight and a decrease in collagen percentage. This recovery in muscle mass, indicative of regeneration, was also observed after the use of acupuncture and electrical stimulation (Su *et al.*, 2016), of BNFD (Brain-derived neurotrophic factor) (Lopes *et al.*, 2017), and after term neurorrhaphy (Liu *et al.*, 2016). This improvement was also observed in the association of beta-agonist clenbuterol with end-terminal neurorrhaphy, were according to a previous study (Fitton *et al.*, 2001), the observed increase in muscle mass may be associated with reduction in protein degradation and muscle atrophy, which may also justify our study results. The data obtained in the percentage of collagen strengthen this aspect, since the connective tissue commonly creates barriers for fusion of newly formed myotubes, which can cause failure in myogenesis (Borisov *et al.*, 2005).

Xing et al(2015), correlated the increase of PaX7 to the restoration of muscle function after peripheral nerve injury and electrostimulation. PAX7 is a marker of satellite cells, which are the main cells responsible for muscle tissue regeneration, and after their activation, such cells express myogenic factors that will act in the differentiation and fusion of myotubes (Judson *et al.*, 2013). In the SFS group, the PAX7 values found suggest an increase in these cells.

In the S and SFS groups, synaptic gutter occupied by nerve terminals were observed, as reported by Sakakima et al (2000), who concluded that this pattern is due to the re-encounter of the nerve terminals with the remaining post-synaptic folds. According to Sakuma et al (2016), the presence of a normal ultrastructural appearance of NMJs after prolonged denervation and reinnervation indicate that motor function failure is not due to the absence of pre or postsynaptic structural elements, but to a failure in the restoration of synaptic function.

In the treatment of PNLs, the use of this sealant has also been observed as easy to use, with good adhesive capacity (Buchaim *et al.,* 2015), and further, this substance type accelerates the surgical practice (Felix *et al.*, 2013). The heterologous sealant has also been used in medicine, with good results in the treatment of bedsores, being easy to apply and leads to decreased pain in patients after the eighth week of use (Gatti *et al.*, 2011).

Our study results allowed us to conclude that there was a reestablishment of the nerve impulse, in addition to axonal regeneration, which was as efficient in the SFS group when compared with the S group, with superior values in the SFS in the lesion area (ischiatic nerve). It is an indicative of a protective effect at the lesion site due to the heterologous fibrin sealant use. It can be considered that the decrease in the number of stitches is able to reduce the trauma caused by the needle, as well as accelerating the surgical practice. So the heterologous fibrin sealant used in nerve reconstruction should be considered after peripheral nerve injury.

Acknowledgements

The authors are grateful to Carlos Roberto Padovani for the statistical expertise and consultation and for the funding provided by FAPESP (2017/06472-2).

Potential Conflict of interest

The authors declare they have no conflict of interest.

Referências Bibliográficas

ASPLUND, M. et al. Incidence of traumatic peripheral nerve injuries and amputations in Sweden between 1998 and 2006. **Neuroepidemiology,** v. 32, n. 3, p. 217-28, 2009. ISSN 1423-0208 (Electronic) 0251-5350 (Linking). Disponível em: <http://www.ncbi.nlm.nih.gov/pubmed/19174611 >.

BAIN, J.; MACKINNON, S.; HUNTER, D. Functional evaluation of complete sciatic, peroneal, and posterior tibial nerve lesions in the rat. **Plastic and reconstructive surgery,** v. 83, n. 1, p. 129-136, 1989. ISSN 0032-1052.

BARROS, L. C. et al. A new fibrin sealant from Crotalus durissus terrificus venom: applications in medicine. **J Toxicol Environ Health B Crit Rev,** v. 12, n. 8, p. 553-71, Oct 2009. ISSN 1521-6950 (Electronic) 1093-7404 (Linking). Disponível em: <http://www.ncbi.nlm.nih.gov/pubmed/20183534 >.

BISCOLA, N. P. et al. Multiple uses of fibrin sealant for nervous system treatment following injury and disease. **J Venom Anim Toxins Incl Trop Dis,** v. 23, p. 13, 2017. ISSN 1678-9199 (Print) 1678-9180 (Linking). Disponível em: <http://www.ncbi.nlm.nih.gov/pubmed/28293254 >.

BONNEMANN, C.; BUSHBY, K. The limb-girdle muscular dystrophies. **Engel AG; Franzini Armstrong A, editors Myology 3rd McGraw-Hill**, p. 1077-1121, 2004.

BORISOV, A. B.; DEDKOV, E. I.; CARLSON, B. M. Abortive myogenesis in denervated skeletal muscle: differentiative properties of satellite cells, their migration, and block of terminal differentiation. **Anatomy and embryology,** v. 209, n. 4, p. 269-279, 2005. ISSN 0340-2061.

BUCHAIM, R. L. et al. Effect of low-level laser therapy (LLLT) on peripheral nerve regeneration using fibrin glue derived from snake venom. **Injury,** v. 46, n. 4, p. 655-60, Apr 2015. ISSN 1879-0267 (Electronic) 0020-1383 (Linking). Disponível em: <http://www.ncbi.nlm.nih.gov/pubmed/25669962 >.

CARTAROZZI, L. P. et al. Mesenchymal stem cells engrafted in a fibrin scaffold stimulate Schwann cell reactivity and axonal regeneration following sciatic nerve tubulization. **Brain research bulletin,** v. 112, p. 14-24, 2015. ISSN 0361-9230.

CHIMUTENGWENDE-GORDON, M.; KHAN, W. Recent advances and developments in neural repair and regeneration for hand surgery. **Open Orthop J,** v. 6, p. 103-7, 2012. ISSN 1874-3250 (Electronic) 1874-3250 (Linking). Disponível em: <http://www.ncbi.nlm.nih.gov/pubmed/22431954 >.

CONFORTIM, H. D. et al. Effects of aging and maternal protein restriction on the muscle fibers morphology and neuromuscular junctions of rats after nutritional recovery. **Micron,** v. 71, p. 7-13, 2015. ISSN 0968-4328.

COULET, B. et al. A comparison of intercostal and partial ulnar nerve transfers in restoring elbow flexion following upper brachial plexus injury (C5-C6±C7). **The Journal of hand surgery,** v. 35, n. 8, p. 1297-1303, 2010. ISSN 0363-5023.
DE OLIVEIRA GONÇALVES, J. B. et al. Effects of low-level laser therapy on autogenous bone graft stabilized with a new heterologous fibrin sealant. **Journal of Photochemistry and Photobiology B: Biology,** v. 162, p. 663-668, 2016. ISSN 1011-1344.

ENGEL, A.; ORAWA, E. Chapter 34: Dystrophinopathies. **Myology,(Aggiungere: McGraw-Hill),** v. 978, 2004.

FELIX, S. P. et al. Comparison between suture and fibrin glue on repair by direct coaptation or tubulization of injured mouse sciatic nerve. **Microsurgery,** v. 33, n. 6, p. 468-77, Sep 2013. ISSN 1098-2752 (Electronic) 0738-1085 (Linking). Disponível em: <http://www.ncbi.nlm.nih.gov/pubmed/23836677 >.

FERREIRA, R. S. Autologous or heterologous fibrin sealant scaffold: which is the better choice? **Journal of Venomous Animals and Toxins Including Tropical Diseases,** v. 20, n. 1, p. 31, 2014. ISSN 1678-9199.

FITTON, A.; BERRY, M.; MCGREGOR, A. Preservation of denervated muscle form and function by clenbuterol in a rat model of peripheral nerve injury. **Journal of Hand Surgery,** v. 26, n. 4, p. 335-346, 2001. ISSN 0266-7681.

FROST, H. K. et al. G-CSF prevents caspase 3 activation in Schwann cells after sciatic nerve transection, but does not improve nerve regeneration. **Neuroscience,** v. 334, p. 55-63, 2016. ISSN 0306-4522.

GASPAROTTO, V. P. et al. A new fibrin sealant as a three-dimensional scaffold candidate for mesenchymal stem cells. **Stem Cell Res Ther,** v. 5, n. 3, p. 78, Jun 10 2014. ISSN 1757-6512 (Electronic) 1757-6512 (Linking). Disponível em: <http://www.ncbi.nlm.nih.gov/pubmed/24916098 >.

GATTI, M. et al. Treatment of venous ulcers with fibrin sealant derived from snake venom. **Journal of Venomous Animals and Toxins including Tropical Diseases,** v. 17, n. 2, p. 226-229, 2011. ISSN 1678-9199.

GAUDET, A. D.; POPOVICH, P. G.; RAMER, M. S. Wallerian degeneration: gaining perspective on inflammatory events after peripheral nerve injury. **J Neuroinflammation,** v. 8, p. 110, Aug 30 2011. ISSN 1742-2094 (Electronic)1742-2094 (Linking). Disponível em: <http://www.ncbi.nlm.nih.gov/pubmed/21878126 >.

GENSEL, J. C. et al. Behavioral and histological characterization of unilateral cervical spinal cord contusion injury in rats. **Journal of neurotrauma,** v. 23, n. 1, p. 36-54, 2006. ISSN 0897-7151.

GERMINARIO, E. et al. Early changes of type 2B fibers after denervation of rat EDL skeletal muscle. **Journal of Applied Physiology,** v. 92, n. 5, p. 2045-2052, 2002. ISSN 8750-7587.

GIORDANI, G. et al. Tratamento da paralisia facial por neurotização. **Arq Catarinenses Med,** v. 38, p. 152-154, 2009.

GORDON, T. Nerve Regeneration: Understanding Biology and Its Influence on Return of Function After Nerve Transfers. **Hand Clin,** v. 32, n. 2, p. 103-17, May 2016. ISSN 1558-1969 (Electronic) 0749-0712 (Linking). Disponível em: <http://www.ncbi.nlm.nih.gov/pubmed/27094884 >.

GORDON, T.; HEGEDUS, J.; TAM, S. L. Adaptive and maladaptive motor axonal sprouting in aging and motoneuron disease. **Neurological research,** v. 26, n. 2, p. 174-185, 2004. ISSN 0161-6412.

GRINSELL, D.; KEATING, C. P. Peripheral nerve reconstruction after injury: a review of clinical and experimental therapies. **Biomed Res Int,** v. 2014, p. 698256, 2014. ISSN 2314-6141 (Electronic). Disponível em: < http://www.ncbi.nlm.nih.gov/pubmed/25276813 >.

HIGASHINO, K. et al. Early changes in muscle atrophy and muscle fiber type conversion after spinal cord transection and peripheral nerve transection in rats. **Journal of neuroengineering and rehabilitation,** v. 10, n. 1, p. 46, 2013. ISSN 1743-0003.

ISAACS, J. E. et al. Comparative analysis of biomechanical performance of available “nerve glues”. **The Journal of hand surgery,** v. 33, n. 6, p. 893-899, 2008. ISSN 0363-5023.

JOHNSON, R. A.; WICHERN, D. W. **Applied multivariate statistical analysis**. Prentice-Hall New Jersey, 2014.

JUDSON, R. N.; ZHANG, R. H.; ROSSI, F. Tissue-resident mesenchymal stem/progenitor cells in skeletal muscle: collaborators or saboteurs? **The FEBS journal,** v. 280, n. 17, p. 4100-4108, 2013. ISSN 1742-4658.

LEHRER, G. M.; ORNSTEIN, L. A diazo coupling method for the electron microscopic localization of cholinesterase. **The Journal of Cell Biology,** v. 6, n. 3, p. 399-406, 1959. ISSN 0021-9525.

LIU, H.-F. et al. Can the Babysitter Procedure Improve Nerve Regeneration and Denervated Muscle Atrophy in the Treatment of Peripheral Nerve Injury? **Plastic and reconstructive surgery,** v. 138, n. 1, p. 122-131, 2016. ISSN 0032-1052.

LOPES, C. D. et al. BDNF gene delivery mediated by neuron-targeted nanoparticles is neuroprotective in peripheral nerve injury. **Biomaterials,** v. 121, p. 83-96, 2017. ISSN 0142-9612.

MACIEL, F. O. et al. Effect of electrical stimulation of the cranial tibial muscle after end-to-side neurorrhaphy of the peroneal nerve in rats. **Acta Cir Bras,** v. 28, n. 1, p. 39-47, Jan 2013. ISSN 1678-2674 (Electronic) 0102-8650 (Linking). Disponível em: <http://www.ncbi.nlm.nih.gov/pubmed/23338112 >.

MALOMOUZH, A. I. Non-cholinergic signaling pathways at vertebrate neuromuscular junctions. In: (Ed.). **Skeletal Muscle-From Myogenesis to Clinical Relations**: InTech, 2012.

MARTINS, R. S. et al. Electrophysiologic assessment of regeneration in rat sciatic nerve repair using suture, fibrin glue or a combination of both techniques. **Arq Neuropsiquiatr,** v. 63, n. 3A, p. 601-4, Sep 2005. ISSN 0004-282X (Print) 0004-282X (Linking). Disponível em: < http://www.ncbi.nlm.nih.gov/pubmed/16172708 >.

MENDONÇA, A. C.; BARBIERI, C. H.; MAZZER, N. Directly applied low intensity direct electric current enhances peripheral nerve regeneration in rats. **Journal of neuroscience methods,** v. 129, n. 2, p. 183-190, 2003. ISSN 0165-0270.

MICHAEL, F. et al. Denervation-induced mitochondrial dysfunction and autophagy in skeletal muscle of apoptosis-deficient animals. **American Journal of Physiology-Cell Physiology,** v. 303, n. 4, p. C447-C454, 2012. ISSN 0363-6143.

NAKAMURA, T. et al. Experimental study on the regeneration of peripheral nerve gaps through a polyglycolic acid-collagen (PGA-collagen) tube. **Brain Res,** v. 1027, n. 1-2, p. 18-29, Nov 19 2004. ISSN 0006-8993 (Print) 0006-8993 (Linking). Disponível em: < http://www.ncbi.nlm.nih.gov/pubmed/15494153 >.

NIKOLAOU, S. et al. Contribution of denervated muscle to contractures after neonatal brachial plexus injury: not just muscle fibrosis. **Muscle & nerve,** v. 49, n. 3, p. 398-404, 2014. ISSN 1097-4598.

OHIRA, T. et al. The effects of heat stress on morphological properties and intracellular signaling of denervated and intact soleus muscles in rats. **Physiological reports,** v. 5, n. 15, p. e13350, 2017. ISSN 2051-817X.

PATTERSON, M. F.; STEPHENSON, G.; STEPHENSON, D. G. Denervation produces different single fiber phenotypes in fast-and slow-twitch hindlimb muscles of the rat. **American Journal of Physiology-Cell Physiology,** v. 291, n. 3, p. 518-528, 2006. ISSN 0363-6143.

PERUSSI BISCOLA, N. et al. Long-standing motor and sensory recovery following acute fibrin sealant based neonatal sciatic nerve repair. **Neural plasticity,** v. 2016, 2016. ISSN 2090-5904.

PINHEIRO-DARDIS, C. M.; RUSSO, T. L. Electrical stimulation based on chronaxie increases fibrosis and modulates TWEAK/Fn14, TGF-β/myostatin, and MMP pathways in denervated muscles. **American journal of physical medicine & rehabilitation,** v. 96, n. 4, p. 260-267, 2017. ISSN 0894-9115.

RAFIJAH, G. et al. The effects of adjuvant fibrin sealant on the surgical repair of segmental nerve defects in an animal model. **J Hand Surg Am,** v. 38, n. 5, p. 847-55, May 2013. ISSN 1531-6564 (Electronic) 0363-5023 (Linking). Disponível em: <http://www.ncbi.nlm.nih.gov/pubmed/23561728 >.

RASBAND, W. **ImageJ. US National Institutes of Health, Bethesda, MD** 1997.

RAY, W. Z.; MACKINNON, S. E. Management of nerve gaps: autografts, allografts, nerve transfers, and end-to-side neurorrhaphy. **Exp Neurol,** v. 223, n. 1, p. 77-85, May 2010. ISSN

1090-2430 (Electronic) 0014-4886 (Linking). Disponível em: <http://www.ncbi.nlm.nih.gov/pubmed/19348799 >.

RICH, M. M.; LICHTMAN, J. W. In vivo visualization of pre- and postsynaptic changes during synapse elimination in reinnervated mouse muscle. **J Neurosci,** v. 9, n. 5, p. 1781-805, May 1989. ISSN 0270-6474 (Print) 0270-6474 (Linking). Disponível em: <https://www.ncbi.nlm.nih.gov/pubmed/2542480 >.

RUVEN, C.; WU, W. Transplantation of embryonic spinal cord derived cells to prevent muscle atrophy after various peripheral nerve injuries. 2017 Hong Kong Inter-University Postgraduate Symposium in Biochemical Sciences, 2017.

SAKAKIMA, H. et al. Effects of short-term denervation and subsequent reinnervation on motor endplates and the soleus muscle in the rat. **Archives of histology and cytology,** v. 63, n. 5, p. 495-506, 2000. ISSN 0914-9465.

SAKUMA, M. et al. Lack of motor recovery after prolonged denervation of the neuromuscular junction is not due to regenerative failure. **Eur J Neurosci,** v. 43, n. 3, p. 451-62, Feb 2016. ISSN 1460-9568 (Electronic) 0953-816X (Linking). Disponível em: <http://www.ncbi.nlm.nih.gov/pubmed/26332731 >.

SCHNEIDER, C. A.; RASBAND, W. S.; ELICEIRI, K. W. NIH Image to ImageJ: 25 years of image analysis. **Nature methods,** v. 9, n. 7, p. 671-675, 2012. ISSN 1548-7091.

SEDDON, H. J. A Classification of Nerve Injuries. **Br Med J,** v. 2, n. 4260, p. 237-9, Aug 29 1942. ISSN 0007-1447 (Print) 0007-1447 (Linking). Disponível em: <http://www.ncbi.nlm.nih.gov/pubmed/20784403 >.

SOBRAL, L. et al. Immediate versus later exercises for rat sciatic nerve regeneration after axonotmesis: histomorphometric and functional analyses. **Brazilian Journal of Physical Therapy,** v. 12, n. 4, p. 311-316, 2008. ISSN 1413-3555.

SU, Z. et al. Acupuncture plus low-frequency electrical stimulation (Acu-LFES) attenuates denervation-induced muscle atrophy. **Journal of Applied Physiology,** v. 120, n. 4, p. 426-436, 2016. ISSN 8750-7587.

SULLIVAN, R. et al. Peripheral Nerve Injury: Stem Cell Therapy and Peripheral Nerve Transfer. **Int J Mol Sci,** v. 17, n. 12, Dec 14 2016. ISSN 1422-0067 (Electronic) 1422-0067 (Linking). Disponível em: < http://www.ncbi.nlm.nih.gov/pubmed/27983642 >.

TINTIGNAC, L. A.; BRENNER, H. R.; RUEGG, M. A. Mechanisms Regulating Neuromuscular Junction Development and Function and Causes of Muscle Wasting. **Physiol Rev,** v. 95, n. 3, p. 809-52, Jul 2015. ISSN 1522-1210 (Electronic) 0031-9333 (Linking). Disponível em: < http://www.ncbi.nlm.nih.gov/pubmed/26109340 >.

TRICAUD, N.; PARK, H. T. Wallerian demyelination: chronicle of a cellular cataclysm. **Cellular and Molecular Life Sciences**, p. 1-9, 2017. ISSN 1420-682X.

TU, H. et al. Morphological Regeneration and Functional Recovery of Neuromuscular Junctions after Tourniquet-Induced Injuries in Mouse Hindlimb. **Front Physiol,** v. 8, p. 207,

2017. ISSN 1664-042X (Print) 1664-042X (Linking). Disponível em: <http://www.ncbi.nlm.nih.gov/pubmed/28428759 >.

TUFFAHA, S. H. et al. Growth hormone therapy accelerates axonal regeneration, promotes motor reinnervation, and reduces muscle atrophy following peripheral nerve injury. **Plastic and reconstructive surgery,** v. 137, n. 6, p. 1771-1780, 2016. ISSN 0032-1052.

UYANIKGIL, Y. et al. Useful Effects of Melatonin in Peripheral Nerve Injury and Development of the Nervous System. **J Brachial Plex Peripher Nerve Inj,** v. 12, n. 1, p. e1-e6, Jan 2017. ISSN 1749-7221 (Print) 1749-7221 (Linking). Disponível em: <http://www.ncbi.nlm.nih.gov/pubmed/28603548 >.

VICENTE, E. J. D. et al. Recuperação funcional do nervo ciático reparado pela cola de fibrina. **HU Revista,** v. 34, n. 1, p. 9-12, 2008. ISSN 0103-3123.

WIBERG, R. et al. Investigation of the expression of myogenic transcription factors, microRNAs and muscle-specific E3 ubiquitin ligases in the medial gastrocnemius and soleus muscles following peripheral nerve injury. **PloS one,** v. 10, n. 12, p. e0142699, 2015. ISSN 1932-6203.

WILLAND, M. P. et al. Daily electrical muscle stimulation enhances functional recovery following nerve transection and repair in rats. **Neurorehabilitation and neural repair,** v. 29, n. 7, p. 690-700, 2015. ISSN 1545-9683.

WU, P. et al. Key changes in denervated muscles and their impact on regeneration and reinnervation. **Neural regeneration research,** v. 9, n. 20, p. 1796, 2014.

XING, H. et al. Electrical stimulation influences satellite cell differentiation after sciatic nerve crush injury in rats. **Muscle & nerve,** v. 51, n. 3, p. 400-411, 2015. ISSN 1097-4598.

ZAR, J. Biostatistical Analysis, 4th Impression, Dorling Kindersley (India) Pvt. **Ltd., Delhi,** v. 110, p. 92, 2009.

Anexos

UNIVERSIDADE ESTADUAL PAULISTA
CAMPUS DE BOTUCATU
FACULDADE DE MEDICINA

unesp

FMB

Ética CEUA

Comissão de Ética no Uso de Animais

Criada através da Portaria DFM nº 611 de 13/12/2012

CERTIFICADO Nº 1172/2016-CEUA

Certificamos que a proposta intitulada **"Comparação entre o uso de sutura e cola de fibrina na interação neuromuscular após Lesão Nervosa Periférica"**, registrada com o n. 1172/2016, sob a responsabilidade de Ana Paula Silveira Leite, orientada pela Profa. Dra. Selma Maria Michelin Matheus, com a colaboração de Carina Guidi Pinto – que envolve a produção, manutenção ou utilização de animais pertencentes ao filo Chordata, subfilo Vertebrata (exceto humanos), para fins de pesquisa científica (ou ensino) – encontra-se de acordo com os preceitos da Lei n. 11.794, de 8 de outubro de 2008, do Decreto n. 6.899, de 15 de julho de 2009, e com as normas editadas pelo Conselho Nacional de Controle de Experimentação Animal (CONCEA), e foi aprovado pela Comissão de Ética no Uso de Animais da Faculdade de Medicina de Botucatu, em reunião de 31/03/2016.

Finalidade	( ) Ensino (X) Pesquisa Científica
Vigência da autorização	01/05/2017
Espécie/Linhagem/Raça	Ratos Wistar
Nº de animais	36
Peso/Idade	300 gramas/60 dias
Sexo	Macho
Origem	Biotério Central da FMB - UNESP

Prof. Dr. Guilherme A. M. Barros
Presidente da CEUA

Kleber Messias Camargo
Kleber Messias de Camargo
Secretário da CEUA

Distrito Rubião Junior, s/nº - Botucatu – S.P. CEP: 18.618-687 Fone: (14) 3880-1608/3880-1609 e-mail secretaria: ceua@fmb.unesp.br